Vol. 48, No. 1 (2026) 166-187, DOI: 10.24874/ti.2119.01.26.03

Tribology in Industry

www.tribology.rs

RESEARCH

Tribological and Performance Analysis of a 4-Stroke Diesel Engine Employing Reduced Graphene Oxide Additive Added into Engine Oil

Emrullah Hakan Kaleli[a,*], Levent Yüksek[a], Selman Demirtaş[a]

[a]Yildiz Technical University, Faculty of Mechanical Engineering, E1 Block, No.28, Beşiktaş-Yıldız-İstanbul, Turkey 34349.

Keywords:

Friction
Roughness
Reduced graphene oxide
Diesel engine

* Corresponding author:

Emrullah Hakan Kaleli
E-mail: kaleli@yildiz.edu.tr

Received: 21 January 2026
Revised: 24 February 2026
Accepted: 6 March 2026

A B S T R A C T

As the tribological behaviour of a commercialized, fully synthetic 5W40 engine oil upon the incorporation of reduced graphene oxide in sample (0.02 wt.%) like (5W40 engine oil+ 0.02 wt.% Reduced Graphene Oxide) called rGO6 presented superior tribological properties by exhibiting the lowest COF value in our previous work, the same sample was evaluated through a reciprocating tribometer, using steel ball (100 CR6) on a real polished Diesel engine cylinder liner with 5W-40 engine oil to investigate their wear and friction behaviour in boundary lubrication regime. Successful dispersion stability of engine oil added with graphene was also evaluated through an engine dynamometer test. It was found that a rGO6 nano-additive played an active role in lowering the coefficient of friction (%3.29) and increased surface protection by forming a protective layer on a smooth nanorough on rubbing surfaces in both triple repeated tribometer and engine tests increasing engine power by %13.51 and engine torque by %12.00.

1. INTRODUCTION

Lubricants play an essential role in the efficient performance of an engine, and additives contained in the lubricating oil can either enhance or reduce the properties of the base oil. Improvements in nanotechnology have demonstrated the potential for nanoparticle additives to improve the thermal properties of such lubricants. Recent studies have also shown that nanoparticles can work to improve the performance of lubrication. As such, there has been an interest in dispersing nanoparticles in base lubricants to obtain suspensions referred to as nano lubricants [1-4].

The use of nano-additives improves the performance of lubricants by minimizing energy loss due to friction and wear. The invention of internal combustion engines has greatly improved human production efficiency. Friction and wear are key factors in the quest for engine machine fuel efficiency because one-third of the fuel energy is consumed by friction [5]. The friction loss sources of the average passenger car were identified and classified according to the tribological contact and lubrication mechanism. Friction in tribocontacts was estimated according to prevailing contact mechanisms such as electrohydrodynamic,

hydrodynamic, mixed, and boundary lubrication. Coefficients of friction in the tribocontacts were estimated based on available information in the literature on the average passenger car in use today, a car with today's advanced commercial tribological technology, a car with today's best advanced technology based upon recent research and development [6].

Graphene is a rapidly rising star on the horizon of materials science and condensed-matter physics. This strictly two-dimensional material exhibits exceptionally high crystal and electronic quality, and, despite its short history, has already revealed a cornucopia of new physics and potential applications. It is the name given to a flat monolayer of carbon atoms tightly packed into a two-dimensional (2D) honeycomb lattice and is a basic building block for graphitic materials of all other dimensionalities. More generally, graphene represents a conceptually new class of materials that are only one atom thick, and, on this basis, offers new inroads into low-dimensional physics that has never ceased to surprise and continues to provide a fertile ground for applications [7].

Graphene, just like the structured MoS_2, is a 2-D layered material with sp2 -bonded carbon, that has received substantial attention [8-10] due to its good conductivity, excellent mechanical properties, potential applications in electrochemical energy storage [11], microelectronics, and lubricating additives [12].

With the development of nanotechnologies, the use of nano-additives added to base oils has been shown to reduce friction and wear due to their excellent lubricating effects. Graphene has excellent mechanical properties with a low coefficient of friction and wear resistance and has a wide range of tribological applications. However, the stable dispersion of graphene in lubricating media is challenging. In recent years, graphene has received extensive attention owing to its excellent electrical, thermal, mechanical, electrochemical, and optical properties. Graphene has also attracted great attention in the field of lubrication owing to its excellent mechanical properties, coupled with its unique low coefficient of friction and wear resistance [13,14]. Graphene has considered to be one of the most promising and attractive lubricating nanomaterials. It is an excellent candidate material for solid lubricants and lubricant additives and has great potential in tribological applications [15,16].

The maximum energy efficiency for an ideally operating engine is about 85%, but a typical internal combustion engine delivers only 25% of the input fuel energy to the transmission system, this leaves the field open for improvements [17]. Only 12% of the available energy in the fuel finds its way to the driving wheels, with some 15% being dissipated as mechanical, mainly frictional, losses. The worldwide economic implications of this are startling and the prospect of significant improvement in efficiency by modest reductions in friction are apparent. A 10% reduction in mechanical losses would lead to a 1.5% reduction in fuel consumption [18].

Reduction of friction in mechanical elements is one of the most important factors for improving energy efficiency of machine, enhancing the durability of the components and minimizing the emission of harmful gases in the environment [19].

Tribology is based on the study of lubrication, friction and wear at macro level. Nanotribology deals with the variation in properties of lubricants and contacting surfaces at micro/nano level. The term "nano-lubricant" in the present context represents a lubricant which is used for nano applications, or a lubricant obtained by the addition of nanoparticles [3]. In the present study nano-lubricant is tested to represent Reduced Graphene Oxide nanoparticle as the additive. The lubrication characteristics of oil containing (rGO) reduced graphene oxide nanoparticle in Diesel engine oil have been evaluated. (GO) graphene oxide (100 mg) synthesized by a modified Hummers method was reduced by a mixture of glacial acetic acid and hydroiodic acid (AcOH/HI). In a typical procedure, a volume of 20 mL (10 g) from the engine oil was added in a clean vial (22 mL). Then, rGO was added in different mass ratios (0.02% – 0.01%), and the mixture was homogenized for 30 min, through an ultrasound assisted process. We are very thankful to Dr. Minas M. Stylianakis and his team for dispersion and evaluation of the mixture [20]. As a result of the present work, the possible advantage arising from the nanoparticle embodiment in the lubricating oil, which is meant to provide friction and wear reduction, was demonstrated with tribometer and engine test rGO.

2. EXPERIMENTAL DETAILS

Figure 1 (a, b) shows 5W40 reference oil and the prepared "hybrid" nano lubricant 5W-40 containing 0.02 wt % rGO, remained stable for more than 6 months as mentioned in our previous work [1], while it resulted in lower COF compared to the reference 5W-40 engine oil by 3.29%, as estimated with the use of a tribometer. New tests for the current study were confirmed using steel ball (100 CR6) on a real polished gasoline engine cylinder liner specimens specially cut for tribometer tests. In the meantime, engine dynamometer tests were also carried out with the same material. Figure 1(c, d, e) shows 5W40 reference oil 5W-40 containing 0.02 wt % rGO in suspension for engine test. It should be noted that friction tests were conducted according to the active standard test method (ASTM) G181 [21], attesting antifriction and antiwear properties of rGO when embedded in lubricants.

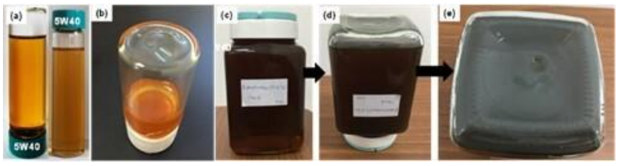

Fig. 1. (a) 5W40 reference oil (b,c,d) colloidal form of rGO+5W40 sample No6 (0.02%wt) still in suspension after 6 months.

Tribometer tests presented that a graphene nano-additive rGO (0.02 wt.%) played an active role in lowering the coefficient of friction and increasing surface protection and lubrication by forming a protective layer on the rubbing surfaces. This is due to the polishing effect by the nanoparticles which is an interaction between the nanoparticles in the oil and the asperity on the surface of the specimen that makes the surface smoother providing nano roughness. As the polishing effect increases, the friction coefficient decreases. This reduces the frictional heat, thus maintaining a higher viscosity compared with the raw oil. Therefore, the oil film is preserved at high load.

2.1 Tribometer and engine tests

Tribological performance of the dispersed reduced graphene oxide was performed with 5W-40 synthetic multigrade engine oil, provided by Shell Co. (Turkey) (Table 1), is fully synthetic, enriched by very low contents (confidential) of some chemical elements such as Ca, Zn, P, S and Mg. Its specifications conform to API SN/CF; ACEA A3/B3, A3/B4; BMW LL-01; MB 229.5, 226.5; VW 502.00/505.00; Porsche A40; Renault RN0700, RN0710; PSA B71 2296, Ferrari; Fiat 9.55535-Z2 and Chrysler MS-10725, utilizing a customized reciprocating tribometer setup, as shown in Figure 2. The tribometer is driven by a servomotor, and 800 data (values) per second were collected from the load cell, using a data logger, directly connected to a monitor. Our load cells force sensor is provided from ESIT electronic company in Istanbul-TURKEY. It is SPA platform type load cell that can measure weights from a single point. It offers a high level of accuracy and features internal thermal compensation that corrects output drifts due to ambient temperature variations. It is resistant to momentum forces. Our SPA load cell is produced at 3kg, and it is mounted in the center of the platform. Each stroke lasted 0.8 s (640 data per second) and in this way the average CoF of the wear track during the measurement was estimated. All tests were carried out under boundary lubrication conditions at 100 °C. Normal load during the tribological measurements was set to be 60.5 N. Sliding speed or reciprocating velocity and stroke were 0.055 m/s and 8 mm, respectively. The temperature of the block was set up to 100 °C, using an advanced heater, equipped with a digital controller mounted on the setup. To run a 21 min tribotest measurement, three drops (3cc) from engine oil were dropped on the surface of the polished liner specimens. Then, the 100CrMn6 steel ball rubbed on it under boundary lubrication conditions, as displayed in Figure 3. Data acquisition was done by specific software, developed using MATLAB, which was programmed to filter any vibrational noise and to calculate the average CoF, by plotting the final CoF curve, as a function of time. In this set-up, the liner slides against a stationary ball.

Table 1. The properties of 5W-40 synthetic engine oil.

Some Properties of 5W-40 synthetic engine oil	
Total Base Number (TBN)	11.28 mg KOH/g
Flash point	217 °C
Viscosity @100 °C	13.59 cSt
Viscosity @40 °C	84.27 cSt

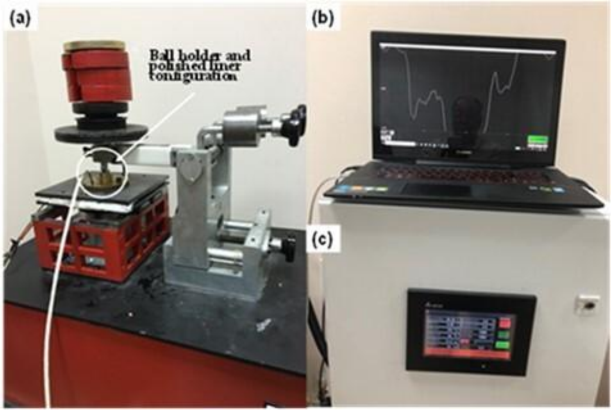

Fig. 2. Reciprocating tribotest setup: (a) general view, (b) recording of accurate friction force data measurement, (c) heating and temperature control and monitoring.

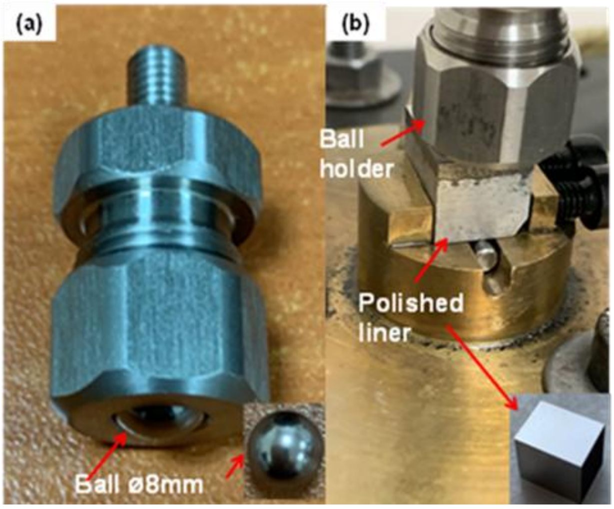

Fig. 3. Ball and liner specimen configuration: (a) Ball placed in the holder, (b) Ball holder and liner integrated configuration.

Figure 4 shows Anadolu Motor Antor 6 LD 400 Diesel engine test setup. Engine performance tests were repeated 3 times and the average was taken. The speed is determined according to ISO 8178-4 standard. As seen in Figure 5, intermediate speed according to ISO 8178 standard; the speed (showed with the number 3) is the maximum torque that occurs.

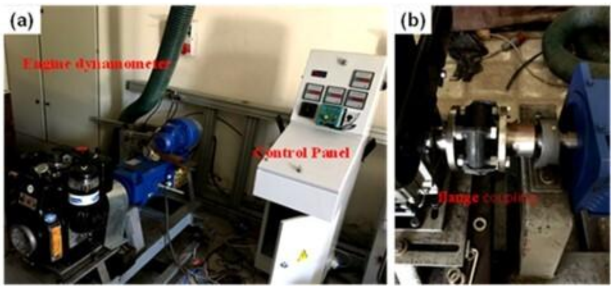

Fig. 4. Anadolu Motor Antor 6 LD 400 Diesel engine test setup (a) dynamometer (b) flange coupling.

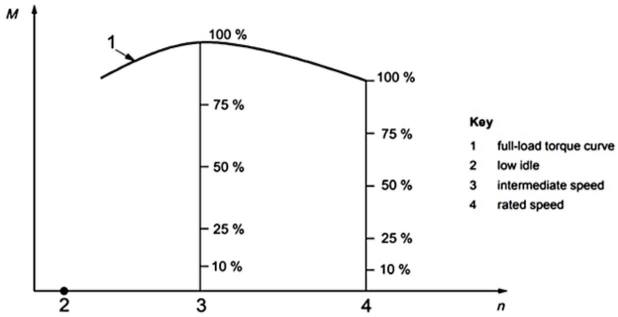

Fig. 5. Speed detection for engine life testing according to ISO 8178-4 standard.

Power: P= IxV Torque: T= ((Px9550))/n,
P: Power (KW), I: Amper, V: Volt, Torque (Nm), n(rev/min)

2.2 Preparation of cylinder liner specimens for tribotest

Anadolu Motor 6LD400 Diesel engine and its technical specifications to be used for experimental work and its technical specifications are presented in Figure 4. It is air cooled and single cylinder engine.

Anadolu Motor Antor 6 LD 400 Diesel engine and its technical specifications to be used for experimental work and its technical specifications are presented in Figure 6. It is air cooled and single cylinder engine.

Engine	Specification
Model diesel	6 LD 400
Cylinder volüme	395 cm^3
Cylinder diameter	86 mm
Compression ratio	18.1
Max. speed	3600 rpm
Max. power	8.5 HP
Max. torque	2 kgm @2200 d/dk
Fuel capacity	4.5 lt
Fuel consumption	220 gr/HP/hour
Oil consumption	13 gr/ hour
Oil capacity	1.2 lt
Dry weight	45 kg

Fig. 6. Anadolu Motor Antor 6 LD 400 Diesel engine and its technical specifications to be used for Tribometer tests.

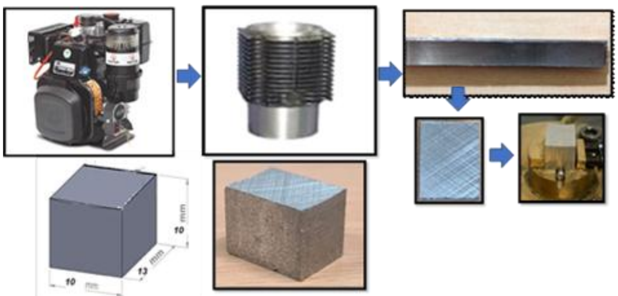

Fig. 7. Cutting cylinder barrel of Diesel engine and mounting in tribometer.

The cylinder barrel test specimens were cut accurately by dry cutting method. The cutting process is performed accurately in Dünya Kalıp limited using CNC milling process technology in Istanbul TURKEY without damaging the honed surfaces. It has considered the substrate temperature and controlled the temperature during the cutting process due to possible material property changes at cylinder–liner substrates induced by heat. During the cutting process, surface temperature was controlled by infrared digital thermometer and measurements showed that surface temperature had not exceeded 49°C. The cylinder–liner substrates dimensions were 10 mm x 13 mm x 10 mm (w x l x h) as presented in Figure 7.

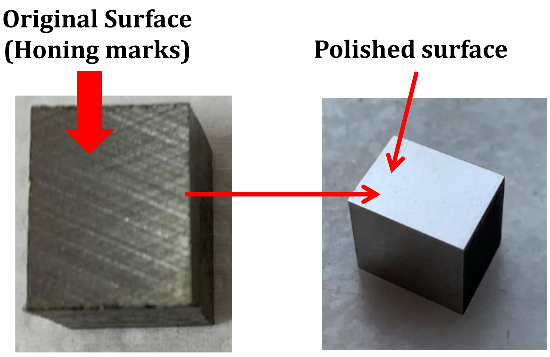

Fig. 8. Polished surface after Cutting cylinder liner.

Figure 8 presents polished surface of plateau honing marks after cutting process. The surface is well polished to eliminate the effect of roughness of honing marks as liner is produced conical and elliptical in its cold state [22].

2.3 Preparation of cylinder liner specimens after engine tests

Figure 9 shows the cutting of the cylinder sleeves using the metal cutting device without damaging the surface at the end of the engine tests.

Fig. 9. At the end of the engine tests, the cylinder sleeves were cut on the metal cutting device without damaging the surface.

Figure 10 shows Top Dead Center region where the most wear occurs; this region was examined microscopically.

Fig. 10. Top Dead Center region of the cut cylinder sleeve.

Figure 11 presents optical digital image of non-tested ball. Table 2 shows chemical composition of the non-tested ball, which is low alloy martensitic chrome steel, AISI 52100 steel ball (100 Cr6). Figure 12 presents optical digital image of the non-tested and polished liner. The liner material of this engine is a grey cast iron. Chemical analysis (analyzed at 01.12.2016) of cylinder material given by Anadolu Engine Group for Antor LD400 Diesel engine is given in table 3.

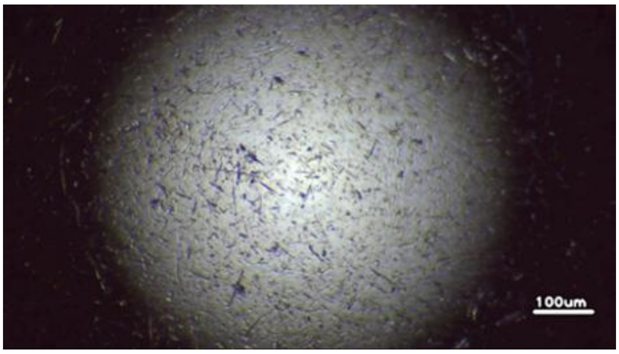

Fig. 11. Non-tested Ball.

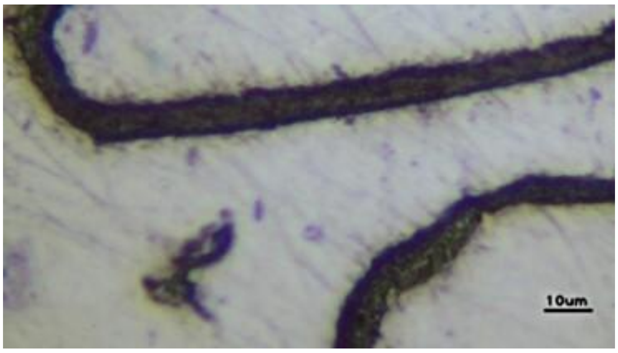

Fig. 12. Non-tested and polished cylinder liner.

Table 2. Chemical composition of the ball100 Cr6 non tested.

Sample Name	%C	%Si	%Mn	%P	%S	%Cr	%Ni	%Mo	%Cu
Low alloy martensitic chrome steel, AISI 52100 (100 Cr6)	0.95-1.05	0.15-0.35	0.25-0.45	0.025 max	0.025 max	1.40-1.65	0.30 max	0.08 max	0.20 max

Table 3. Chemical analysis of cylinder material (grey cast iron).

Element	%	Element	%	Element	%
Carbon C	3.2000	Silicon (Si)	2.59000	Iron (Fe)	92.44082
Phosphorous (P)	0.33319	Sulphur (S)	0.02737	Manganese (Mn)	0.70000
Molibdenum (Mo)	0.02700	Nickel (ni)	0.01900	Chromium (Cr)	0.43700
Cobalt (Co)	0.00343	Copper (Cu)	0.11600	Aluminum (Al)	0.00010
Titanium (Ti)	0.08497	Vanadium (V)	0.01401	Niobium (Nb)	0.00297
Tin (Sn)	0.00359	Magnesium (Mg)	0.00045	Wolfram (W)	0.00010

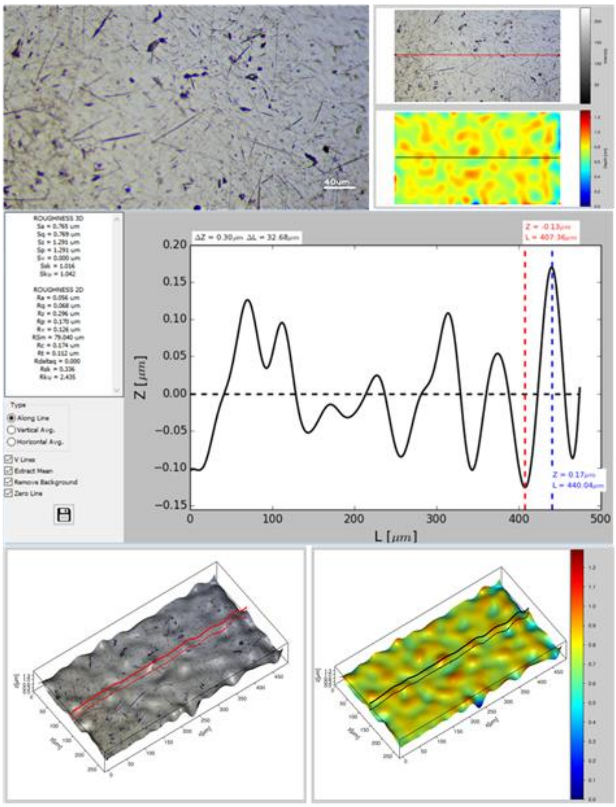

Fig. 13. 2D and 3D roughness of the non-tested ball.

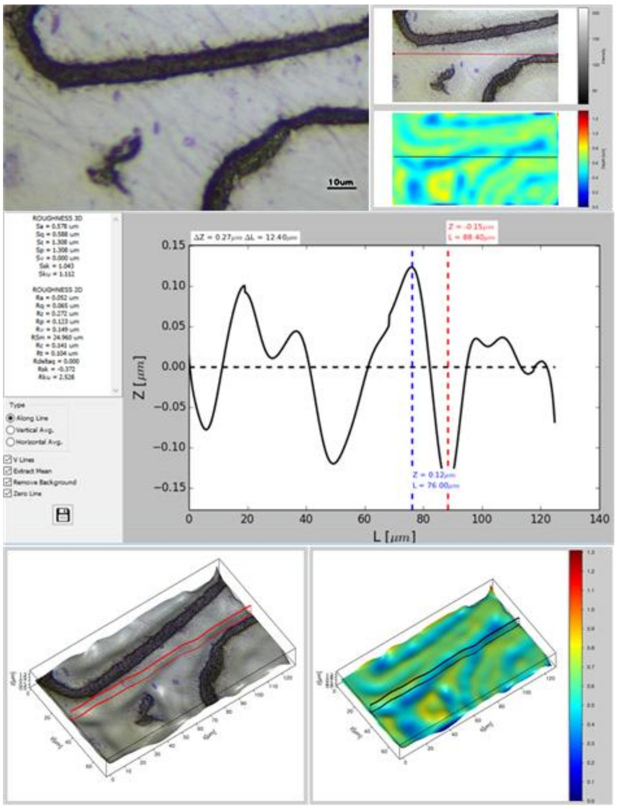

Fig. 14. 2D and 3D roughness of the non-tested and polished cylinder liner.

The hardness of the abrasive ball is max. 207 HB.

Surface analysis of the balls and liner sliding pairs has been carried out through a fully digital optical microscope where 2D-3D roughness and Morphology characterization were performed using a Nanobender 3D HR optical profilometer, with resolution 6400/rotation equipped with a -P-CAMn camera (2MP). All roughness measurements were carried out with X10 Olympus objective choosing high quality removing background section in software. Ra and Sa values were considered for comparison. 2D/3D roughness parameters can be seen clearly in figures as they are less than 1 μm (item no 336 polishing for Ra from 0.0125 μm to 0.26 μm and Rz from 0.25μm to 1.6μm in Microsurf series of comparators) which conforms well with UKAS (National Accreditation Body for the United Kingdom) as mentioned in The Microsurf Series Of Comparators - Rubert & Co Ltd. Figures 13 and 14 show 2D and 3D roughness of the non-tested ball and cylinder liner.

3. RESULTS AND DISCUSSIONS

Tribometer tests were performed of a steel ball on a Diesel engine cylinder liner using a fully formulated oil with and without reduced graphene oxide nano-additive in the boundary lubrication condition. It was found that a rGO nano-additive played an active role in lowering the coefficient of friction and increasing surface protection and lubrication by forming a protective layer on the rubbing surfaces. Tests were carried out three times, and the results were presented for sure results.

3.1 Tribometer test results

Figure 15 presents optical digital images of the wear scar diameter (measured horizontally and vertically) of the (a,c,e) balls tested with reference oil (5w40), (b,d,f) balls tested with rGO added oil. Tests were repeated three times. (a,b) are first test, (c,d) are second and (e,f) are third test.

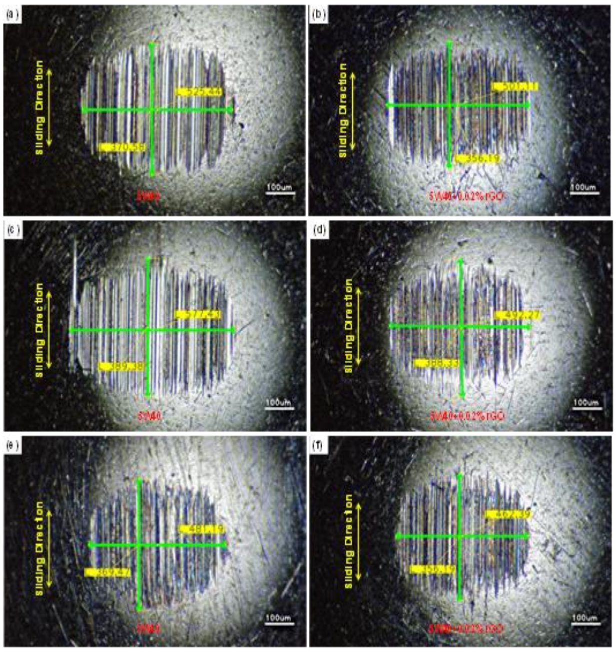

Fig. 15. Optical digital images of the wear scar diameter of the balls tested 3 times on the 3 similar polished cylinder liner. (a,c,e) balls tested with reference oil (5w40), (b,d,f) balls tested with rGO added oil.

As seen in table 4, wear scar diameter of the ball presented lower value horizontally and vertically on rGO6 related to the 5W40 reference oil for each test 1, 2 and 3.

Table 4. Wear scar diameter of the balls tested on the polished Diesel Liner with 5W40 and rGO6.

Test no	Wear scar diameter Horizontally (µm)	Wear scar diameter Vertically (µm)
Test1 (5W40)	525.44	370.58
Test1 (rGO6)	**501.11**	**356.19**
Test2 (5W40)	577.43	389.38
Test2 (rGO6)	**492.27**	**388.33**
Test3 (5W40)	481.19	369.47
Test3 (rGO6)	**462.39**	**356.19**

Figures 16 and 17, Figures 18 and 19 and Figures 20 and 21 show 2D-3D roughness digital optical microscopy of the first, second and third tested ball with reference oil and rGO added oil rubbed on the polished cylinder liner, respectively.

Roughness parameters such as Sa and Ra values were found smaller in rGO added in oil related to the reference oil for three tests as presented in table 5. Abrasion lines are visible on the rubbed wear scar.

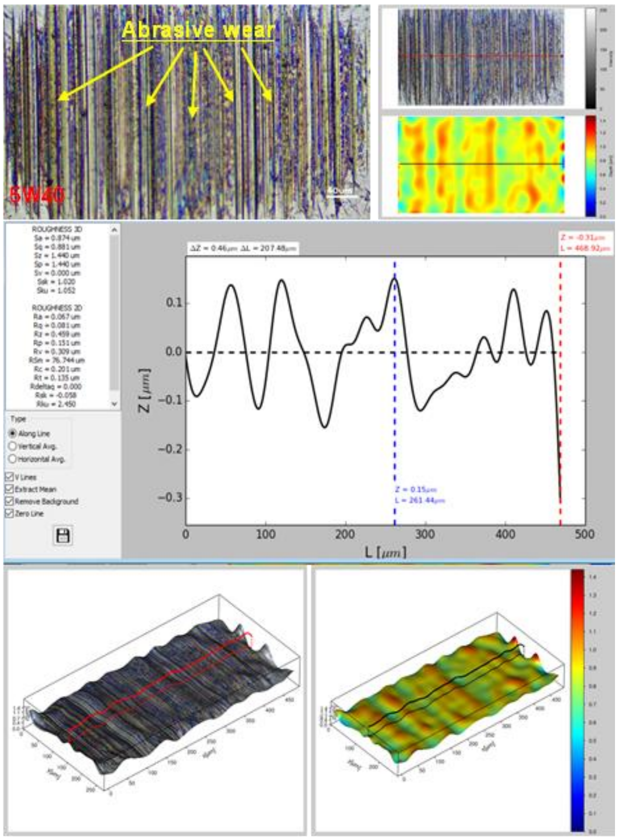

Fig. 16. 2D and 3D roughness of the first tested ball with reference oil rubbed on the polished cylinder liner.

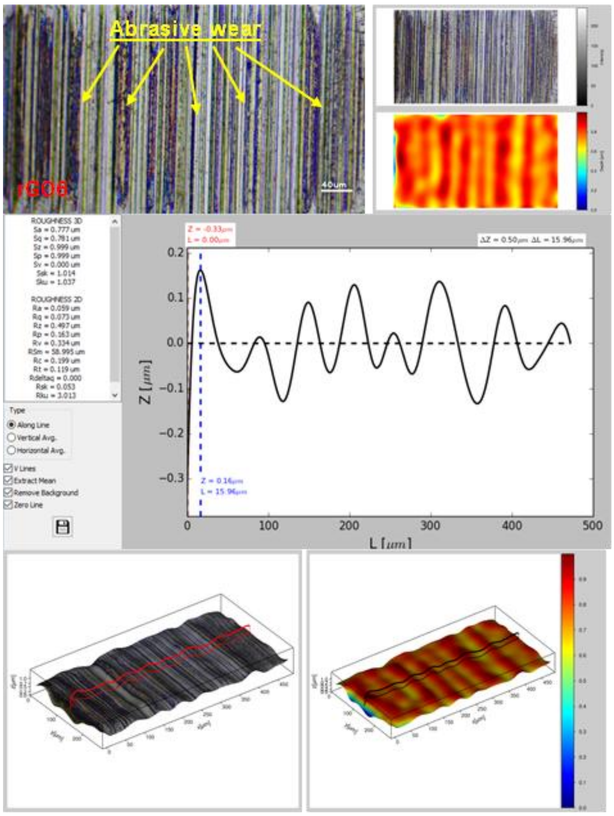

Fig. 17. 2D and 3D roughness of the first tested ball with rGO added oil rubbed on the polished cylinder liner.

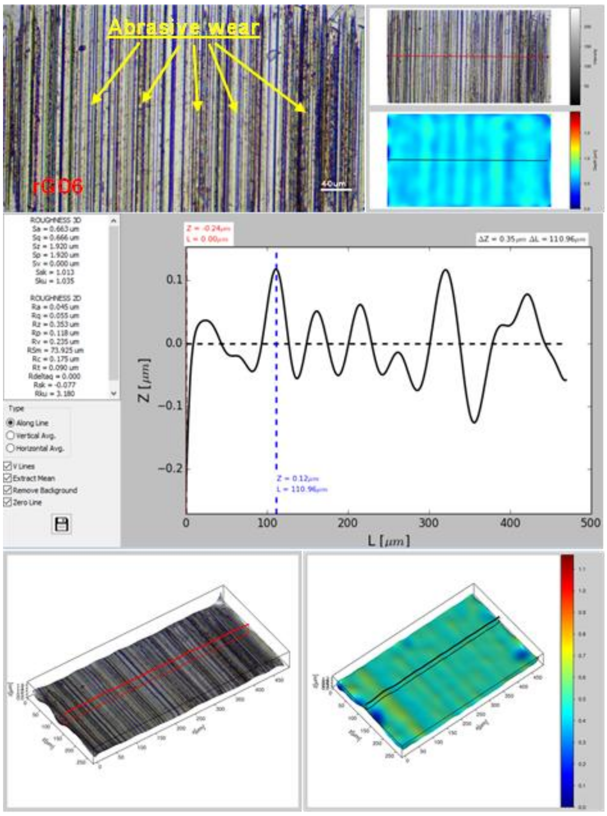

Fig. 19. 2D and 3D roughness of the second tested ball with rGO added oil rubbed on the polished cylinder liner.

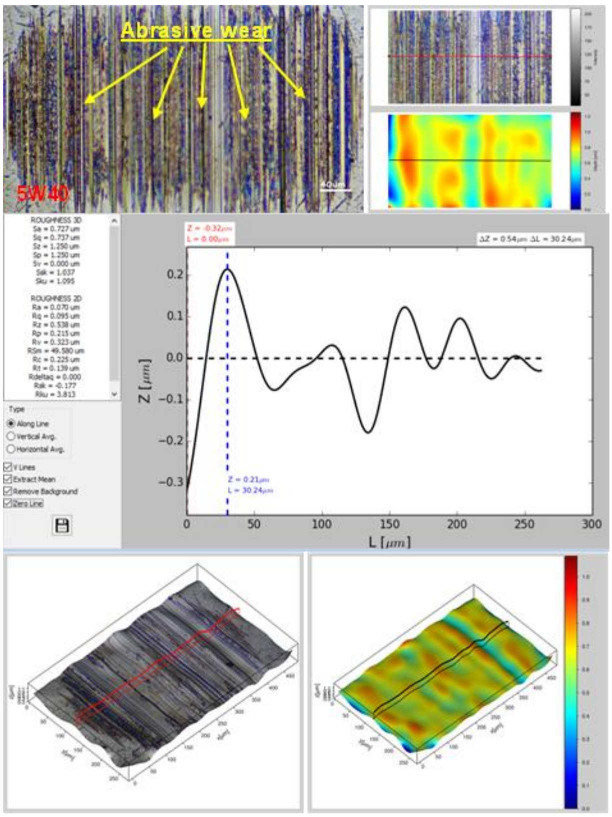

Fig. 18. 2D and 3D roughness of the second tested ball with reference oil rubbed on the polished cylinder liner.

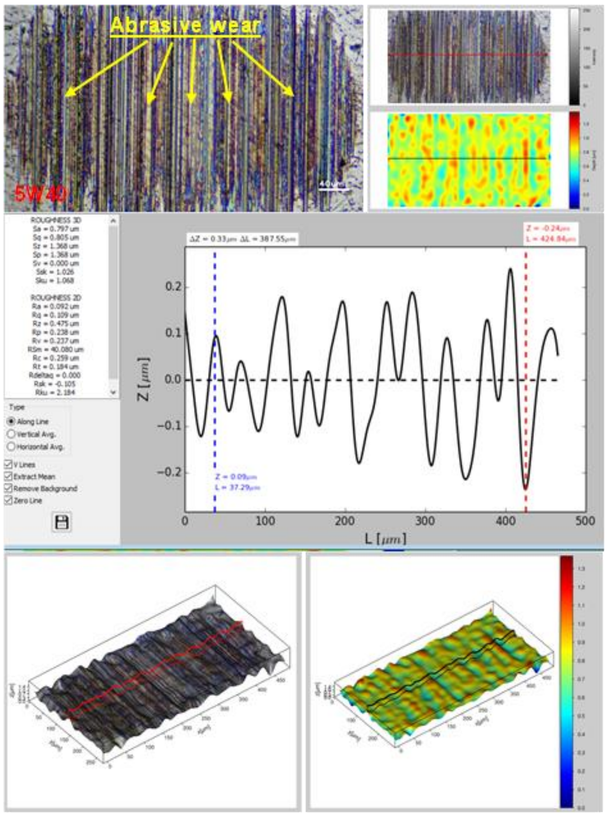

Fig. 20. 2D and 3D roughness of the third tested ball with reference oil rubbed on the polished cylinder liner

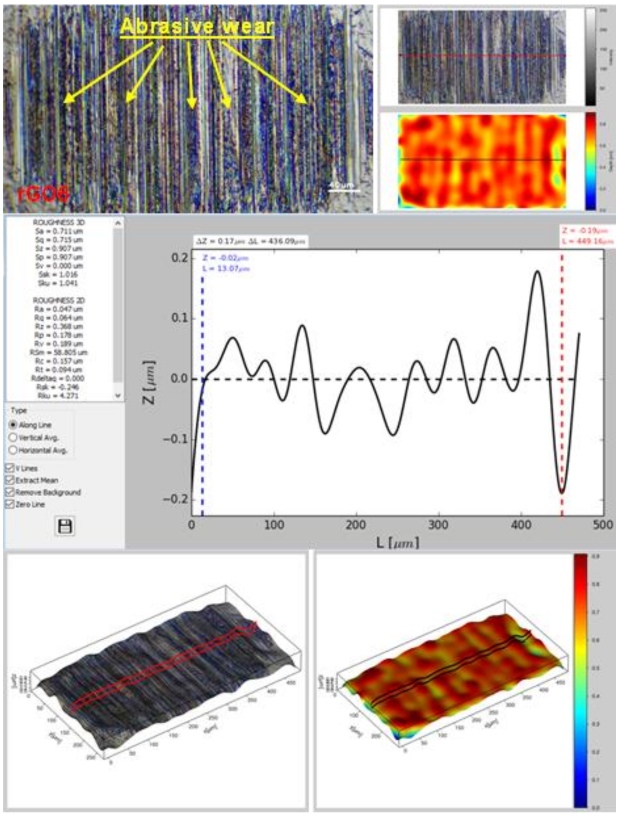

Fig. 21. 2D and 3D roughness of the third tested ball with rGO added oil rubbed on the polished cylinder liner.

Table 5. 2D and 3D roughness value of the wear scar of the balls tested on the polished engine Liner with 5W40 and rGO6.

Test no	Sa (µm)	Ra (µm)
(Non tested ball)	**0.765**	**0.056**
Test1 (5W40)	0.874	0.067
Test1 (rGO6)	**0.777**	**0.059**
Test2 (5W40)	0.727	0.070
Test2 (rGO6)	**0.663**	**0.045**
Test3 (5W40)	0.797	0.092
Test3 (rGO6)	**0.711**	**0.047**

Figure 22 presents the optical digital images of the maximum and minimum wear scar width of the polished engine liner tested 3 times under stell ball. (a,b) are first test, (c,d) are second and (e,f) are third test. As seen in table 6, maximum and minimum wear scar width presented lowest values of the engine Liner tested under steel ball on rGO6 related to the 5W40 reference oil for each test 1, 2 and 3.

Figures 23 and 24, Figures 25 and 26 and Figures 27 and 28 show 2D and 3D roughness of the first second and third tested polished liners with reference oil and rGO added oil rubbed under steel ball, respectively.

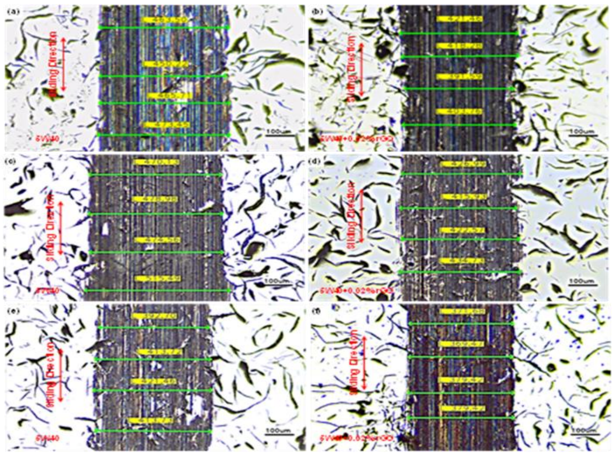

Fig. 22. Optical digital images of the wear scar width of the polished engine liner tested 3 times under stell ball.(a,c,e) liners tested with reference oil (5w40), (b,d,f) liners tested with rGO added oil.

Table 6. Maximum and minimum wear scar width of the polished engine liner tested under steel ball with 5W40 and rGO6.

Test no	Max. wear scar width (µm)	Min. wear scar width (µm)
Test1 (5W40)	473.45	450.22
Test1 (rGO6)	**421.46**	**391.59**
Test2 (5W40)	515.49	470.13
Test2 (rGO6)	**434.73**	**415.93**
Test3 (5W40)	421.46	392.70
Test3 (rGO6)	**379.42**	**369.47**

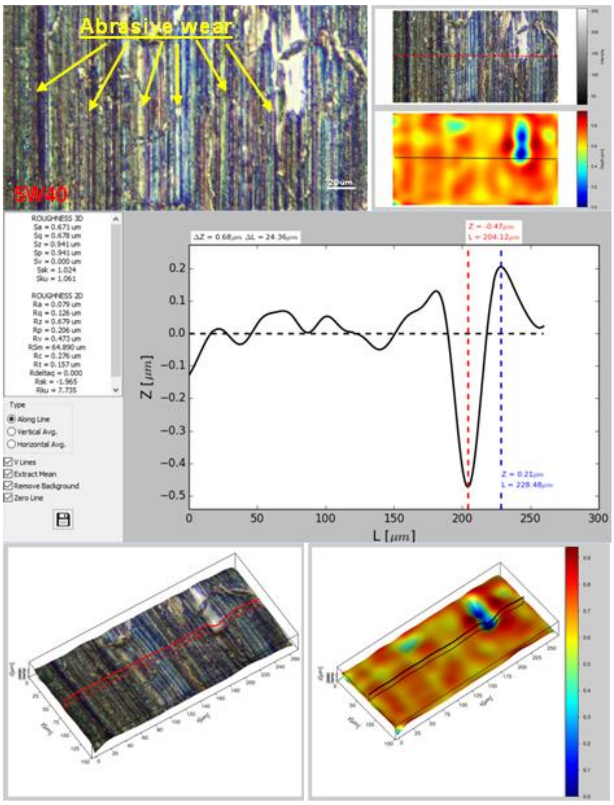

Fig. 23. 2D and 3D roughness of the first tested polished liner with reference oil rubbed under steel ball.

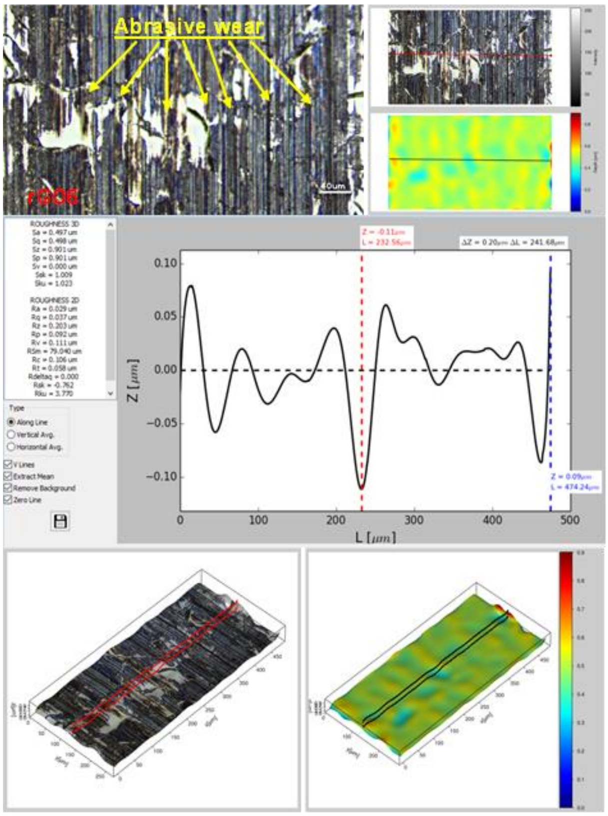

Fig. 24. 2D and 3D roughness of the first tested polished liner with rGO oil rubbed under steel ball.

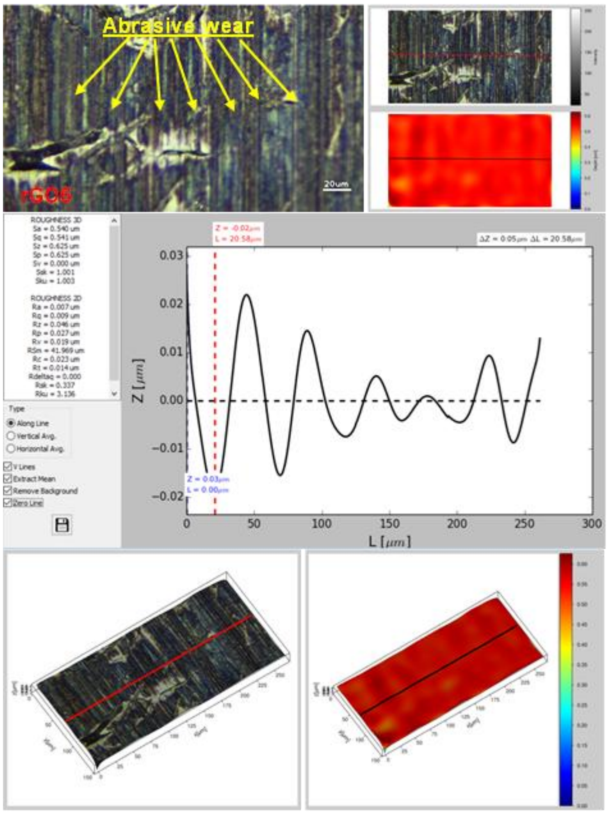

Fig. 26. 2D and 3D roughness of the second tested polished liner with rGO oil rubbed under steel ball.

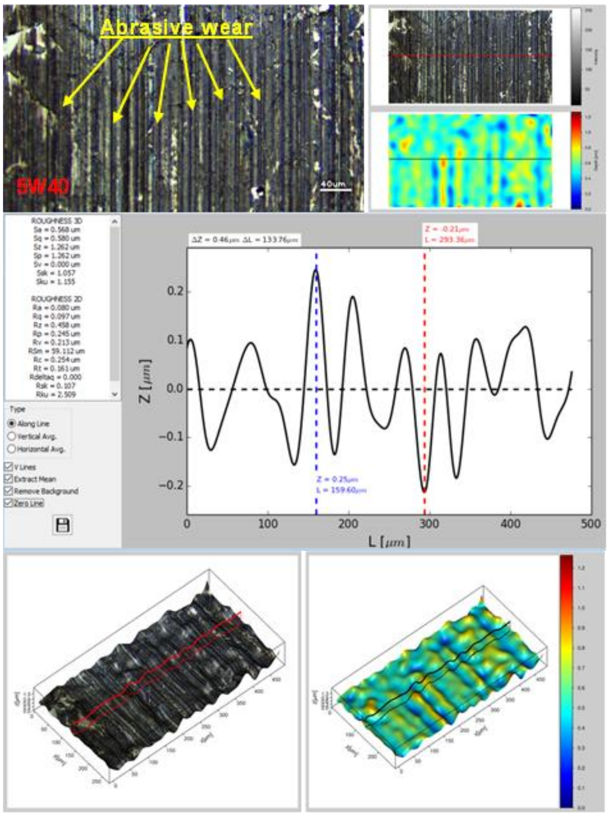

Fig. 25. 2D and 3D roughness of the second tested polished liner with reference oil rubbed under steel ball.

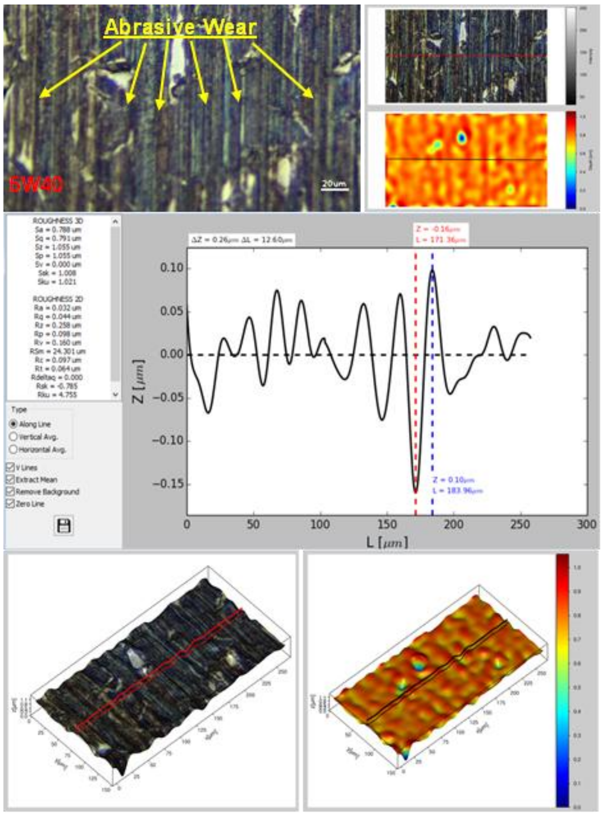

Fig. 27. 2D and 3D roughness of the third tested polished liner with reference oil rubbed under steel ball.

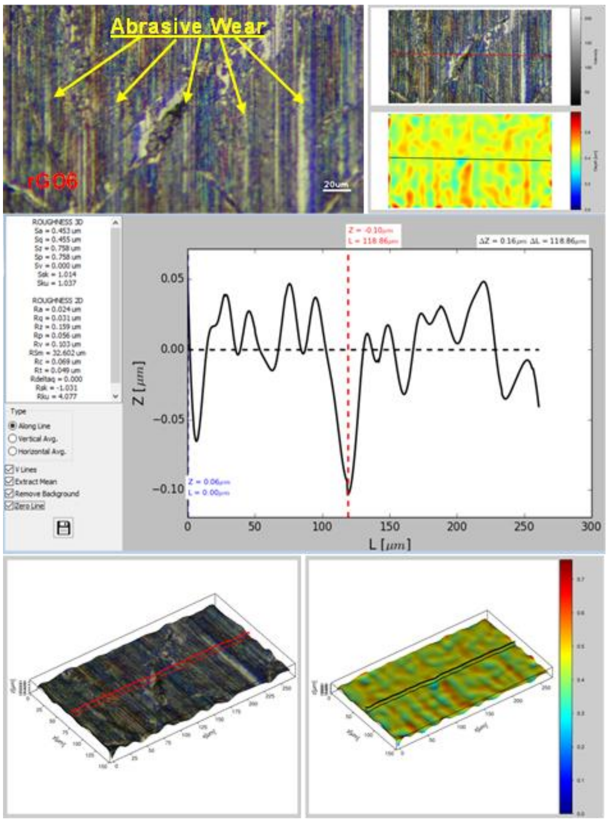

Fig. 28. 2D and 3D roughness of the third tested polished liner with rGO oil rubbed under steel ball.

Roughness parameters such as Sa and Ra values were found smaller in rGO added oil related to the reference oil for three tests as presented in table 7. Abrasion lines are visible on the rubbed wear scar.

Table 7. 2D and 3D roughness value of the wear scar width of the polished Diesel engine Liner tested under steel ball with 5W40 and rGO6.

Test no	Sa (μm)	Ra (μm)
Non tested polished liner	**0.578**	**0.052**
Test1 (5W40)	0.671	0.079
Test1 (rGO6)	**0.497**	**0.029**
Test2 (5W40)	0.568	0.080
Test2 (rGO6)	**0.540**	**0.007**
Test3 (5W40)	0.788	0.032
Test3 (rGO6)	**0.453**	**0.024**

Figure 29 presents 2D-3D roughness digital optical microscopy of the rGO protective layer formed on the tested polished liner with rGO added oil rubbed under steel ball as showed in red circles in a high magnification. Roughness values Sa and Ra are 4.585 μm and 8nm, repectively.

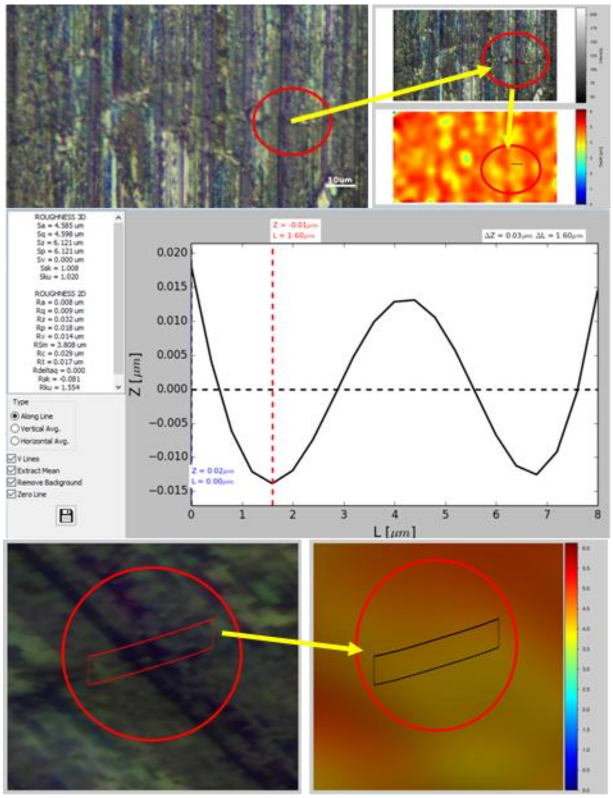

Fig. 29. 2D and 3D roughness of the rGO protective layer formed on the tested polished liner with rGO added oil rubbed under steel ball.

It is also important to observe the wear, scars and grooves on the surfaces of the balls and polished liners. To evaluate the changes in topography during the lubrication tests, an atomic force microscope (Nanosurf Flex AFM), which enables observations of topographic features in 2D and 3D, was employed.

Figure 30 and 31 presents 2D and 3D AFM images of the surfaces of the non-tested ball and polished liners, of he balls and liners tested with reference oil and rGO added oil. Roughness parameters such as Sa and Ra values (as nm) were found smaller in rGO added oil related to the reference oil for 3 magnifications 90 μm X90 μm, 30 μm X30 μm and 5 μm X5 μm as presented in table 8 and 9.

The roughness of the non-tested ball and polished liner was measured less than ~200 nm, and it had a slightly irregular shape. The 2D and 3D topographic images of the ball and liner tested with reference oil showed peaks and valleys repeated along the rubbed direction. We also observed abrasive lines and adhesive wear visible in Figure 30 (b, e, h) and Figure 31 (b, e, h) on the reference oil tested liner. After the test smoother and shallower peaks and valleys were observed with the rGO nano lubricant as the surface is well degraded.

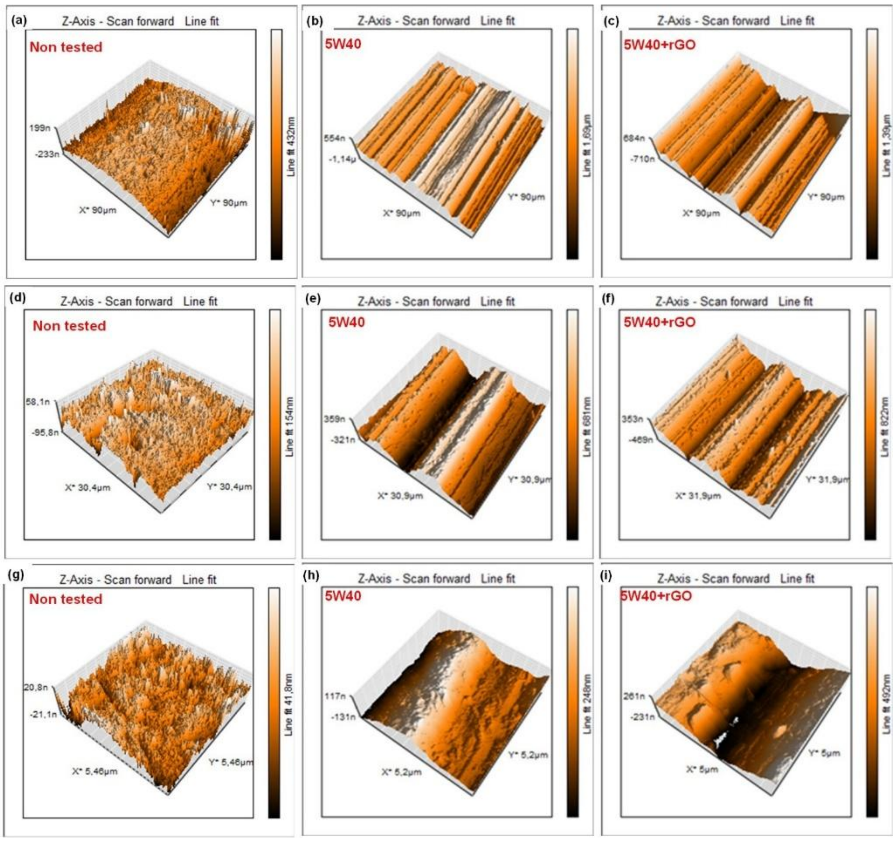

Fig. 30. 2D and 3D AFM images of the surfaces of the non-tested balls (a,d,g) and the ball tested with reference oil (b,e,h) and rGO added oil (c,f,i) rubbed on liner for 3 magnifications 90 µm X90 µm, 30 µm X30 µm and 5 µm X5 µm respectively.

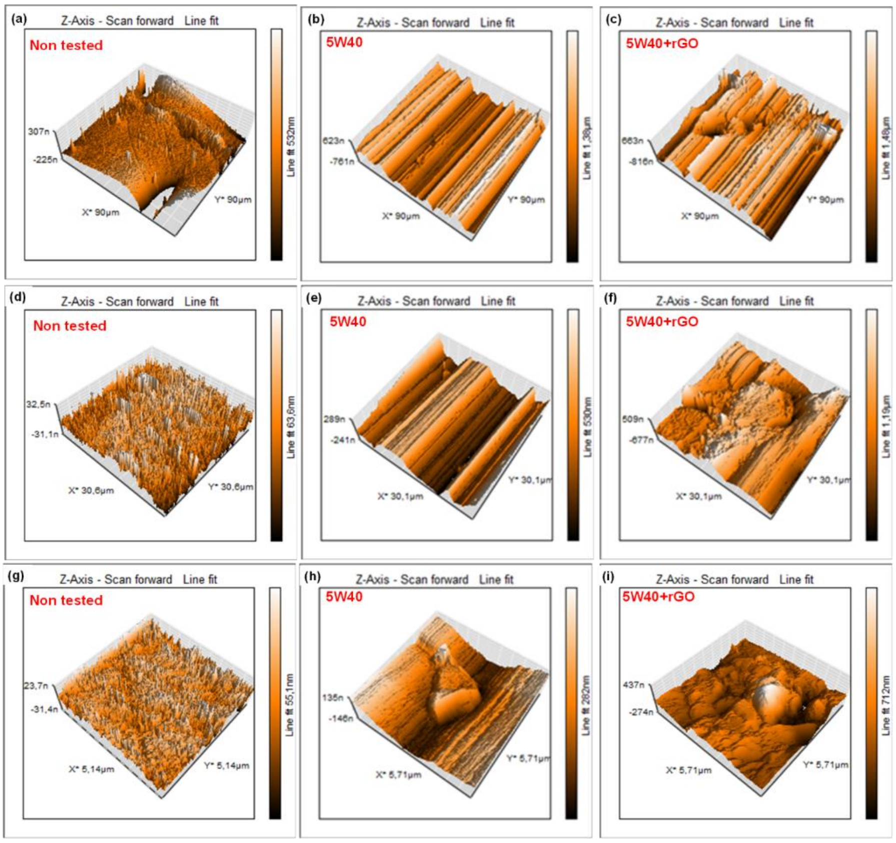

Fig. 31. 2D and 3D AFM images of the surfaces of the non-tested polished liner (a,d,g) and the liner tested with reference oil (b,e,h) and rGO added oil (c,f,i) rubbed under steel ball for 3 magnifications 90 µm X90 µm, 30 µm X30 µm and 5 µm X5 µm respectively.

Taking into account the third test results of ball and liner (tables 4 and 6) where less values of wear scar width has been found, it has also taken SEM-EDX images showing rGO protected well the rubbed surface mixing with additives elements such as Ca, Zn, P and S existing in the reference 5W40 oil. Figures 32, 33, 34 and 35 show SEM images, X-Ray and elemental analysis of the tested surface of the balls and liners. It has been detected carbon element of rGO protective layer for the test of rGO as presented in tables 10 and 11. Abrasion lines are visible on the rubbed wear scar, as usual.

Table 8. 2D-Ra and-3D Sa of AFM roughness value.

AFM (Roughness µm)	Sa (nm)	Ra (nm)
(a) Non tested ball (90 µm X90 µm)	55.998	61.548
(b) Tested ball with 5W40 (90 µm X90 µm)	211.36	206.14
(c) Tested ball with rGO6 (90 µm X90 µm)	**190.87**	**190.02**
(d) Non tested ball (30 µm X30 µm)	16.609	12.849
(e) Tested ball with 5W40 (30 µm X30 µm)	146.41	146.99
(f) Tested ball with rGO6 (30 µm X30 µm)	**114.11**	**115.02**
(g) Non tested ball (5 µm X5 µm)	5.057	4.556
(h) Tested ball with 5W40 (5 µm X5 µm)	46.4	77.13
(i) Tested ball with rGO6 (5 µm X5 µm)	**44.135**	**39.369**

Table 9. 2D-Ra and-3D Sa of AFM roughness value.

AFM (Roughness µm)	Sa (nm)	Ra (nm)
(a) Non tested polished liner (90 µm X90 µm)	72.249	12.137
(b) Tested polished liner with 5W40 (90 µm X90 µm)	242.88	200.39
(c) Tested polished liner with rGO6 (90 µm X90 µm)	**199.86**	**186.75**
(d) Non tested polished liner (30 µm X30 µm)	8.102	6.5525
(e) Tested polished liner with 5W40 (30 µm X30 µm)	150.14	101.79
(f) Tested polished liner with rGO6 (30 µm X30 µm)	**101.08**	**90.034**
(g) Non tested polished liner (5 µm X5 µm)	69.669	31.66
(h) Tested polished liner with 5W40 (5 µm X5 µm)	128.91	121.32
(i) Tested polished liner with rGO6 (5 µm X5 µm)	**47.999**	**28.856**

Shahnazar et al. studied graphite as a lubricant additive for industrial gear oil. They concluded that graphite nanoparticles decreased the metal contact between sliding surfaces by acting as ball bearing spacers [23].

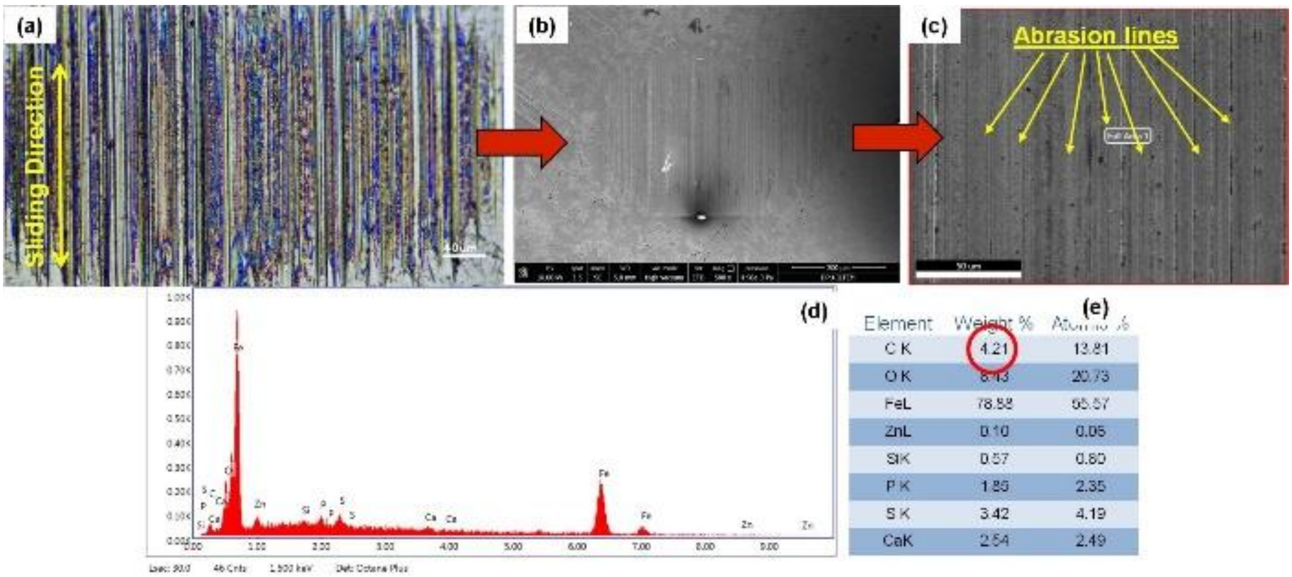

Fig. 32. Ball tested with reference oil (a) optical image, (b,c) S.E.M, (d) X-Ray, (e) elemental analysis.

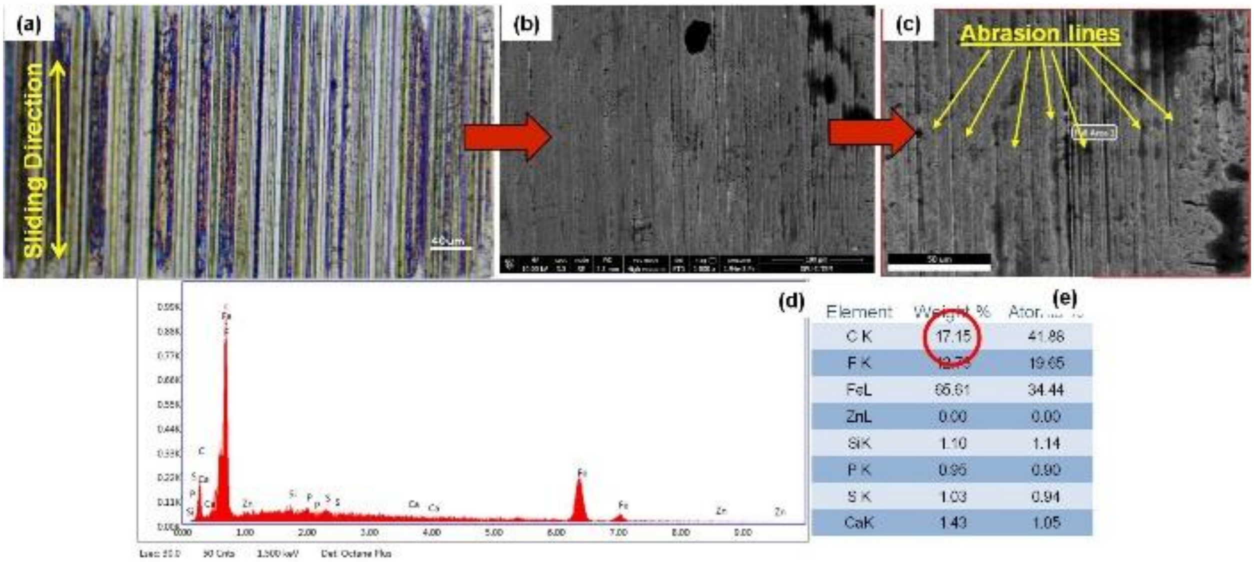

Fig. 33. Ball tested with rGO added oil (a) optical image, (b,c) S.E.M, (d) X-Ray, (e) elemental analysis.

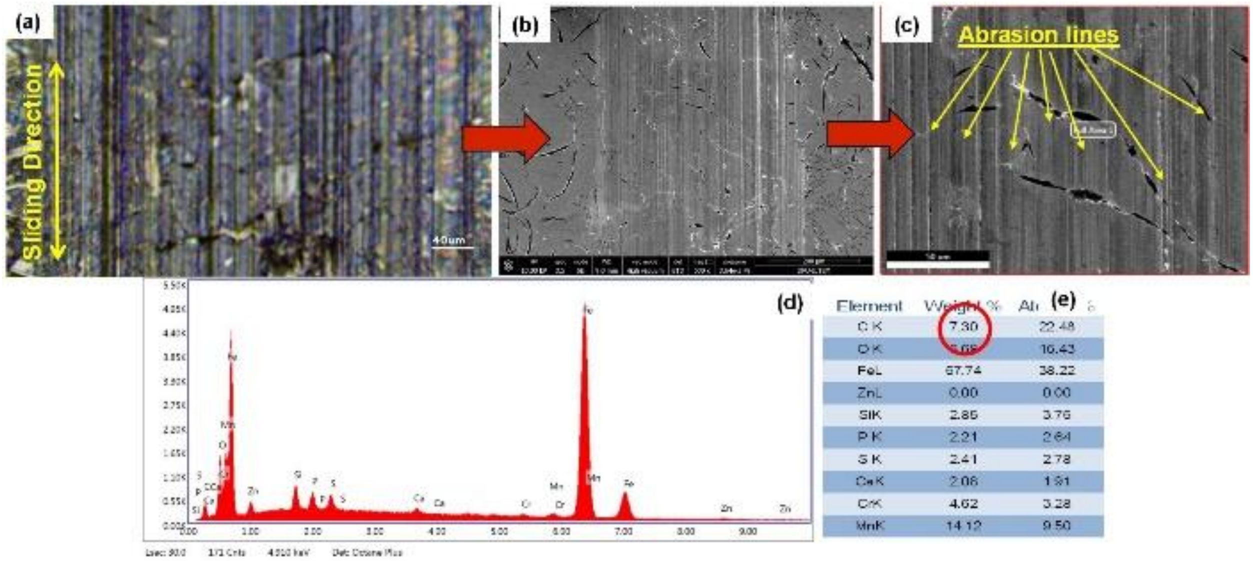

Fig. 34. Liner tested with reference oil (a) optical image, (b,c) S.E.M, (d) X-Ray, (e) elemental analysis.

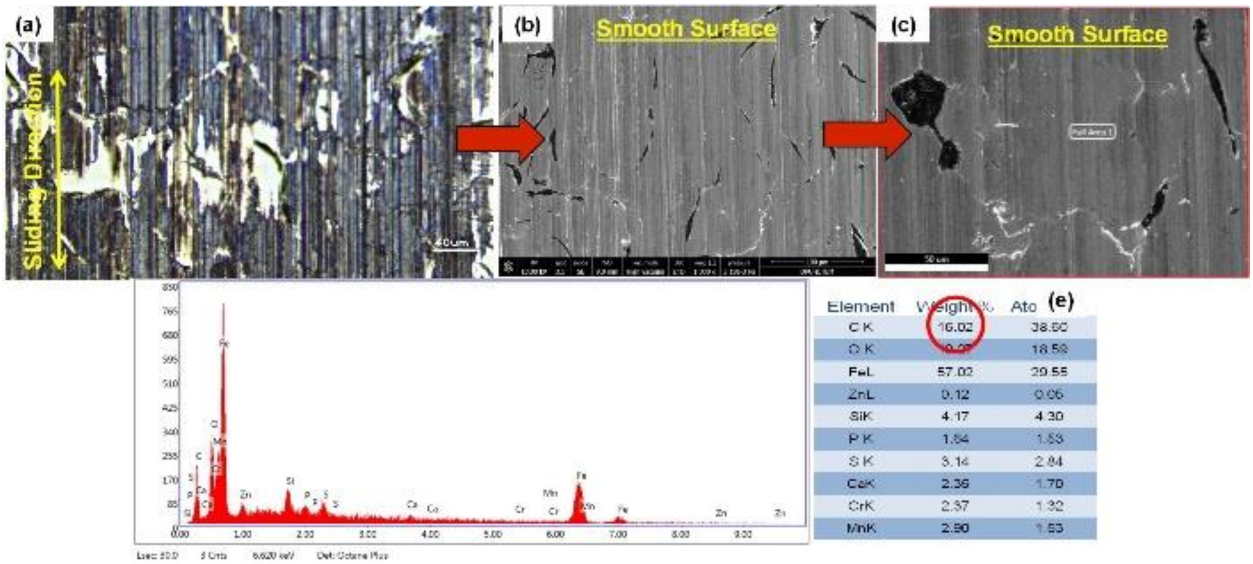

Fig. 35. Liner tested with rGO added oil (a) optical image, (b,c) S.E.M, (d) X-Ray, (e) elemental analysis.

Table 10. Comparison of the elemental analysis of the wear scar of the balls by EDS.

Sample Name	C	O	Fe	Zn	Si	P	S	Ca	Cr	Mn	Total
Wear scar of the ball tested with 5W40	5.29	7.06	69.85	1.04	2.16	1.41	1.50	2.18	5.99	3.51	100
Wear scar of the ball tested with rGO6	11.03	5.65	64.74	1.41	2.60	2.08	2.06	2.64	4.18	3.61	100

Table 11. Comparison of the elemental analysis of the wear scar of the liners by EDS.

Sample Name	C	O	Fe	Zn	Si	P	S	Ca	Total
Wear scar of the liner tested with 5W40	5.06	25.08	45.85	2.36	3.57	5.62	9.06	3.39	100
Wear scar of the liner tested with rGO6	9.68	11.53	49.55	4.03	4.66	5.26	7.84	7.45	100

Chang-Gun, L et al. compared nano lubricants and raw lubricants using a disk-on-disk tribotester, focusing on the influence of the graphite nanoparticle additive. They showed that the addition of graphite nanoparticles to the lubricant enhanced the lubrication characteristics which supports our work. Their morphology analysis indicated that the addition of nanoparticles decreased wear and resulted in a relatively smooth surface with fewer scars, thus indicating that the presence of the graphite nanoparticles significantly reduced metal contact [24].

In literature, the lubricating ability of graphene is most often explained in terms of mechanical effects and its load-carrying capacity. However, the structural evolution and degradation of adsorbed graphene and other carbon nanostructures during tribological operation does not necessarily yield a less effective protective film. This is because accumulated deformation-induced strain or mechanically induced dangling bonds in the nanostructure or its surface functional groups could potentially provide a path to tribofilm formation. Specifically, these structural features may act as tribochemically active sites and react with either tribosurfaces, neighboring nanostructures, wear debris, or other lubricant components. Over time, the accumulation of tribochemical reaction products, nanoparticles, transfer material, and wear debris may become substantial enough to qualify as a proper and strongly bonded tribofilm in accordance with the previously established definition [25].

Xin Kuang et al. studied the performance evaluation of nano-graphene. The advantages make graphene an attractive material for improving the properties of lubricants in a wide range of industrial applications from vehicles, house refrigerators, and industrial machinery such as gearboxes, large compressors, etc. Graphene-based materials are very promising for tribological applications due to their self-lubricating lamellar structure and film-forming abilities, providing excellent anti-wear and friction-reducing performances [26].

Nano-graphene has a unique nanolayered structure, forming a transfer film at the friction interface. Good tribological properties are obtained due to the self-lubrication of graphene by sliding between layers. A large number of basic tribological experiments have found that the addition of an appropriate amount of nano-graphene as a general industrial lubricating oil additive can play a role in reducing friction and wear. In recent years, researchers have begun to study the addition of nano-graphene to engine lubricating oil, mainly focusing on its dispersion stability and tribological properties [27].

Can, O. et al. was observed COF at all concentrations of added GO nanosheets in all lubrication regimes when compared to base engine oil. The obtained results for the boundary lubrication regime ($\lambda < 1.2$) showed that GO nanosheet additives in 0.5, 1, 1.5 and 2.0 mg/mL concentrations reduced the COFs by up to 12.4 %, 13.8 %, 8 % and 13.16 % respectively [28].

Tomanik, E, et al. tested Graphene nanoplatelets, with an average of 9 layers, after functionalization to work as a lubricant additive, reduced both the CoF and friction losses on a reciprocating test. Specifically at the more severe test condition, 40N and 120 °C, the sample L66_2 additive reduced in 5% and 8%, respectively the CoF and the Energy losses in comparison with the reference oil, a fully formulated SAE 0W-20 [29].

Koszalka, G. et al. observed that Graphene-based additives have the potential to increase the efficiency of diesel engines leading to fuel savings and reducing CO2 emissions. However, graphene is a new nanomaterial and there are many unknowns about its properties, as indicated by the significant differences in the results obtained in the studies discussed above. Therefore, its use as a lubricant additive still requires further in-depth study [30].

3.2 Coefficient of fricion results

Figures 36, 37 and 38 are the plotting and average CoF values obtained after experimental reciprocating tribotest of the first, second and third test with reference (5w40) and rGO added oil. Lowest CoF value is obtained with the test of rGO added oil. The horizontal lines represent the average CoF value, which is automatically plotted by the MATLAB assisted specific software of the reciprocating tribotest setup.

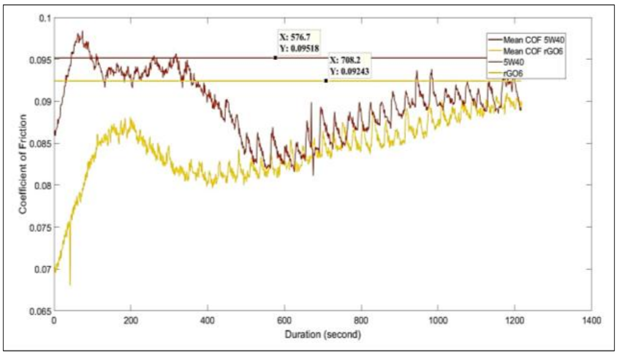

Fig. 36. Plotting and average CoF values obtained after experimental reciprocating tribotest of the first test with reference oil (5w40) and rGO added oil.

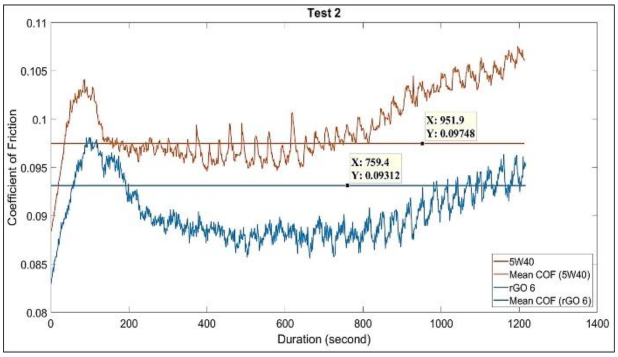

Fig. 37. Plotting and average CoF values obtained after experimental reciprocating tribotest of the second test with reference oil (5w40) and rGO added oil.

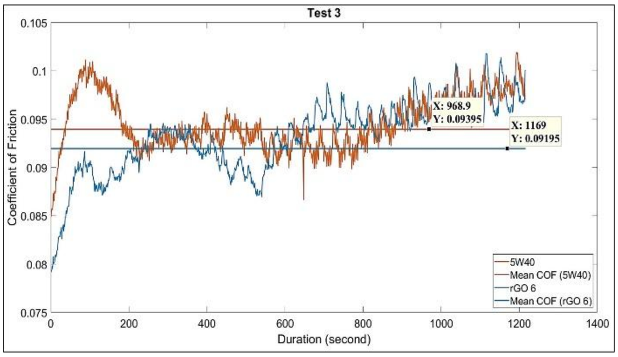

Fig. 38. Plotting and average CoF values obtained after experimental reciprocating tribotest of the third test with reference oil (5w40) and rGO added oil.

Figure 39 presents the average of coefficient of friction data obtained after three repeated tribotests with reference oil (5w40) and rGO added oil. Comparison of COF results were presented in Table 12. The average CoF value exhibited a reduction of 3.29% from reference oil test.

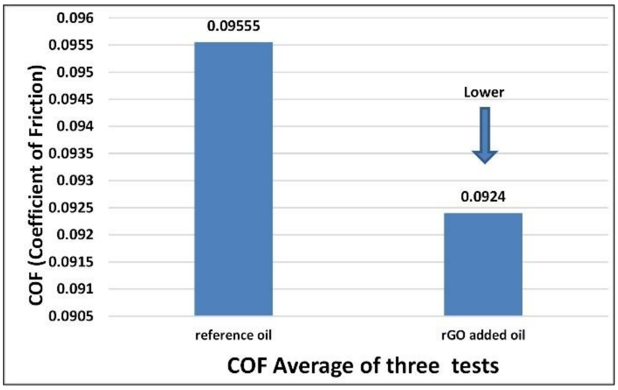

Fig. 39. Average of coefficient of friction data obtained after three repeated tribotests with reference oil (5w40) and rGO added oil. The standard deviation in these data is 1%.

3.3 Engine performance test results

Figure 40 shows engine power test average results repeated 3 times via engine revolution as presented in table 13 and table 14.

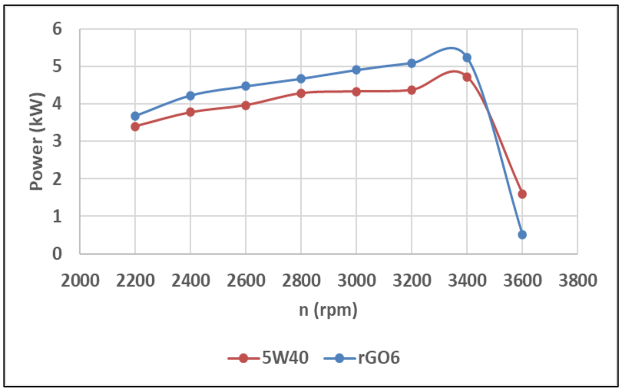

Fig.40. Plotting of Power test results repeated 3 times via engine revolution obtained after experimental engine dynamometer test with reference oil (5w40) and rGO added oil.

Table 12. Comparison of COF results.

Test No	COF 5W40	COF of rGO6
1	0.09518	0.09243
2	0.09748	0.0931
3	0.094	0.0919
Average	0.09555	0.0924

Table 13. Engine Power test results repeated 3 times via engine revolution for reference oil.

	Test 1				Test 2				Test 3				Average	
n(rev/mn)	**V**	**I**	**P**	**T**	**V**	**I**	**P**	**T**	**V**	**I**	**P**	**T**	**P**	**T**
3600	129	13.2	1.7	4.5	128	13.4	1.7	4.5	116	11.9	1.3	3.6	1.5	4.2
3400	215	21.9	4.7	13.2	215	22	4.7	13.2	214	21.9	4.6	13.1	4.7	13.2
3200	207	21.1	4.3	13.0	208	21.1	4.3	13.0	207	21.0	4.3	12.9	4.3	13.0
3000	203	20.9	4.2	13.5	204	21	4.2	13.6	209	21.3	4.4	14.1	4.3	13.7
2800	203	20.8	4.2	14.4	207	21.1	4.3	14.8	205	20.7	4.2	14.4	4.2	14.5
2600	197	20.2	3.9	14.6	201	20.6	4.1	15.2	193	19.5	3.7	13.8	3.9	14.5
2400	189	19.4	3.6	14.5	197	20.2	3.9	15.8	189	19.4	3.6	14.5	3.7	15.0
2200	179	18.4	3.2	14.2	188	19.2	3.6	15.6	179	18.4	3.2	14.2	3.3	14.7

Table 14. Engine Torque test results repeated 3 times via engine revolution for rGO added oil.

	Test 1				Test 2				Test 3				Average	
n(rev/mn)	**V**	**I**	**P**	**T**	**V**	**I**	**P**	**T**	**V**	**I**	**P**	**T**	**P**	**T**
3600	86	8.8	0.7	2.0	83	8.4	0.6	1.8	23	2.4	0.05	0.14	0.5	1.3
3400	231	23.7	5.4	15.3	224	22.3	4.9	14.0	228	22.8	5.1	14.6	5.2	14.6
3200	228	23.3	5.3	15.8	221	22	4.8	14.5	226	22.5	5.0	15.17	5.0	15.1
3000	223	22.6	5.0	16.0	216	21.6	4.6	14.8	224	22.3	4.9	15.9	4.9	15.5
2800	219	22.2	4.8	16.5	210	21	4.4	15.0	218	21.7	4.7	16.1	4.6	15.9
2600	213	21.7	4.6	16.9	209	20.8	4.3	15.9	211	21.0	4.4	16.2	4.4	16.4
2400	207	20.9	4.3	17.2	203	20.5	4.1	16.5	205	20.4	4.1	16.6	4.2	16.8
2200	191	19.3	3.6	16.0	191	19.4	3.7	16.0	191	19.1	3.6	15.8	3.6	15.9

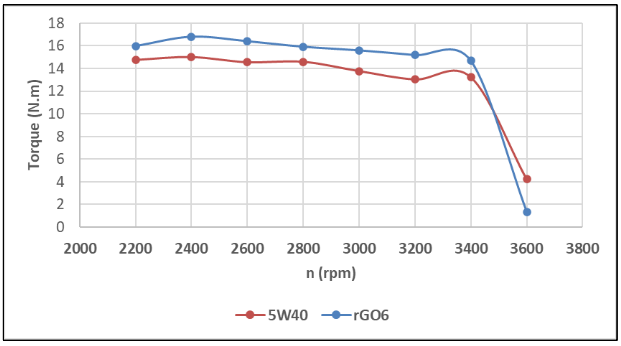

Fig. 41. Plotting of Torque test results repeated 3 times via engine revolution obtained after experimental engine dynamometer test with reference oil (5w40) and rGO added oil.

Figure 41 shows engine torque test average results repeated 3 times via engine revolution as presented in table 13 and table 14.

According to the Power and Torque test results rGO added oil presented higher power and torque performance related to the 5W40 reference oil.

According to the ISO 8178-4 standard, the intermediate speed of the engine was determined to be 2400 rpm. As a result of 3 performance tests performed on a Diesel engine, it was found that rGO-containing oil increased engine power by 13.51% an engine torque by 12.00% compared to the reference oil.

4. SURFACE ANALYSIS OF ENGINE LINERS

Figures 44 and 45 show surface analysis at T.D.C (Top Dead Center) of Diesel engine liner tested with 5W40 and rGO6 oil.

The wear, scars and grooves on the surfaces of the liner at the top dead center was also observed. To evaluate the changes in topography during the lubrication tests, an atomic force microscope (Nanosurf Flex AFM), which enables observations of topographic features in 2D and 3D, was employed.

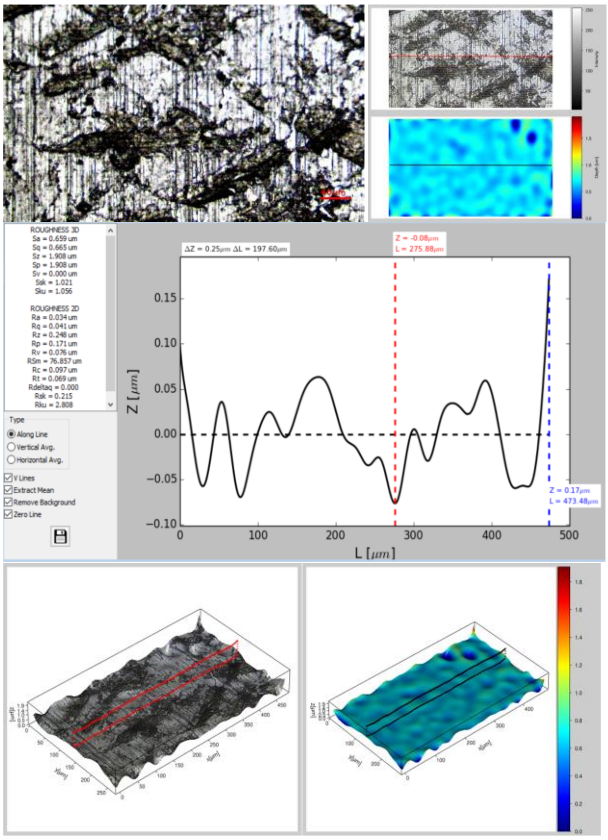

Fig. 42. 2D and 3D roughness of the tested engine liner with 5W40 oil in engine dynamometer.

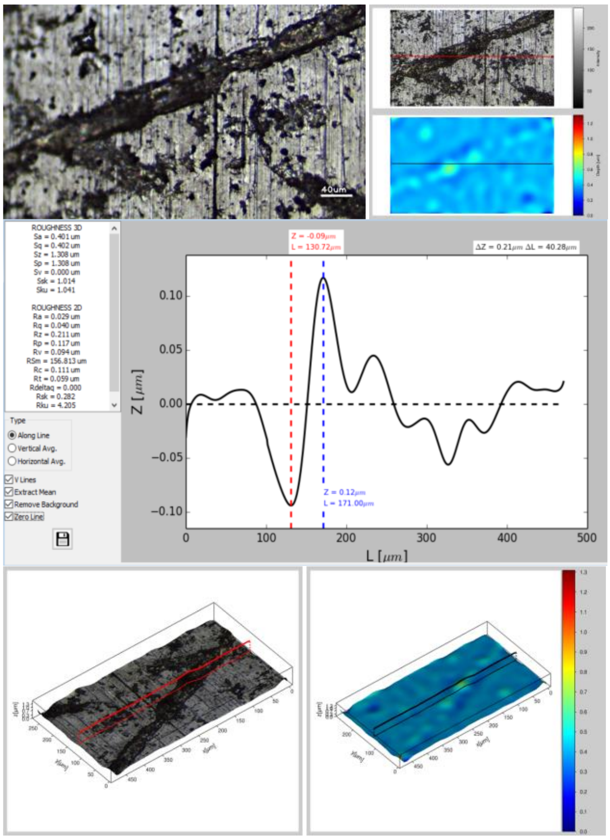

Fig. 43. 2D and 3D roughness of the tested engine liner with rGO added oil in engine dynamometer.

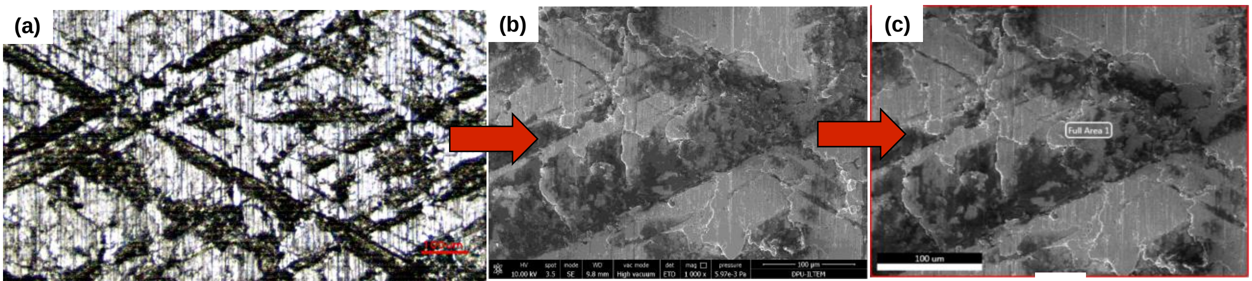

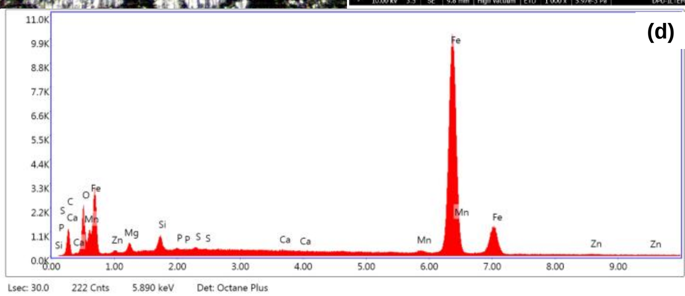

(e)

Element	Weight %	Atomic %
C K	9.21	28.80
O K	5.32	12.49
MgK	0.72	1.11
SiK	0.87	1.17
P K	0.02	0.02
S K	0.07	0.09
CaK	0.22	0.20
MnK	1.04	0.71
FeK	81.93	55.08
ZnK	0.60	0.35

Fig. 44. Surface analysis at T.D.C (Top Dead Center) of Diesel engine linertested with 5W40 oil a) Optical Microscope, b) and c) Electron microscope d) X-Ray e) Elemental analysis.

Figures 42 and 43 show 2D and 3D roughness of the tested engine liner with 5W40 oil and rGO added oil in engine dynamometer. It is usual that the surface (Figure 43) is darker for rGO test than the reference oil (Figure 42) as there is nano graphene effect and protection on the surface.

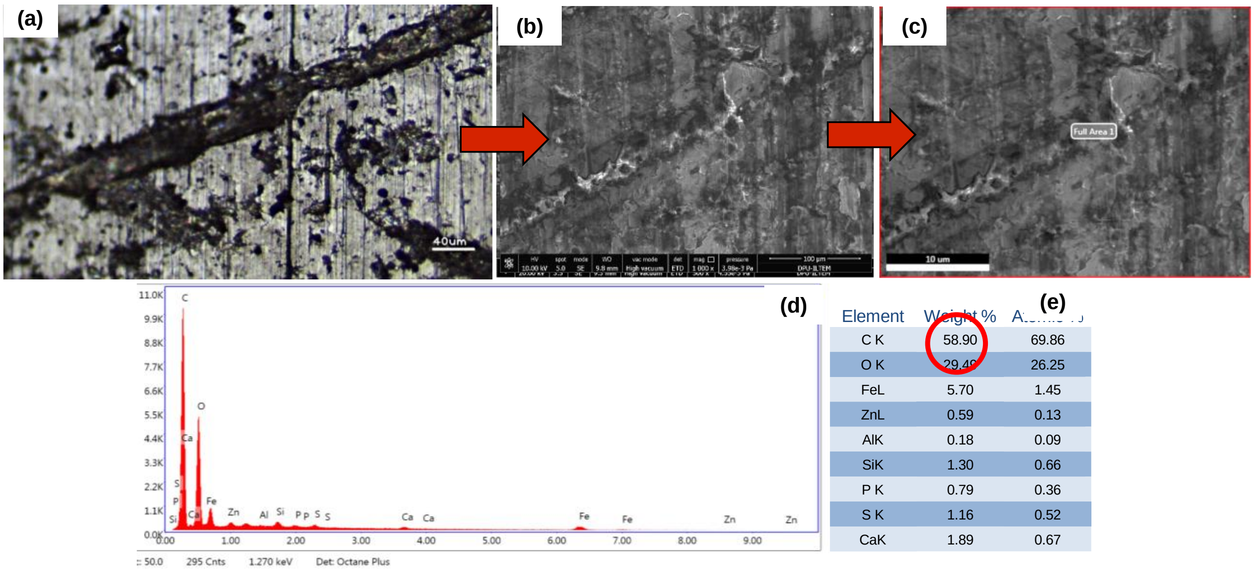

Fig. 45. Surface analysis at T.D.C (Top Dead Center) of Diesel engine liner tested with rGO6 oil a) Optical Microscope, b) and c) Electron microscope d) X-Ray e) Elemental analysis.

Figure 46 presents 2D and 3D AFM images of the surfaces of the non-tested liner, liner tested with reference oil and rGO added oil at the top dead center. Roughness parameters such as Sa and Ra values (as nm) were found smaller in rGO added oil related to the reference oil for 3 magnifications 90 µm X90 µm, 30 µm X30 µm and 5 µm X5 µm as presented in table 15.

The roughness of the non-tested liner was measured less than ~200 nm, and it had a slightly irregular shape. The 2D and 3D topographic images of the liner tested with reference oil showed peaks and valleys repeated along the rubbed direction. We also observed abrasive wear lines visible in (b, e, h) on the reference oil tested liner. After the test smoother and shallower peaks and valleys were observed with the rGO nano lubricant as the surface is well degraded.

To discuss; the concentration of rGO additives in the lube is an important aspect for controlling the friction and wear of the lubricated solid contacts. At lower and higher concentration, the lubrication is ineffective, producing higher friction and wear. However, in optimized concentration 0.02 wt.% of rGO in lube medium showed extremely lower value of friction coefficient 0.09243 and wear reduced up to 3.29% as compared to reference oil without rGO concentration steel-iron contact. Moreover, at high contact pressure, the energy efficiency of optimized rGO additives is improved. This is related to effective shearing of graphene well dispersed in reference oil 5W40 of low shear strength boundary film. Therefore, effective lubrication properties are described by freely suspended boundary tribofilm formation without agglomeration The nanographene particles showed bonding under the contact stress, low shear strength of interlayer sheets easily slides, providing effective lubrication. They become superior at high contact pressure, reducing the friction significantly and more importantly deformation of the wear tracks becomes negligible.

Table 15. 2D-Ra and-3D Sa AFM roughness value.

AFM (Roughness µm)	Sa (nm)	Ra (nm)
(a) Non tested polished liner (90 µm X90 µm)	12,137	72,249
(b) Tested polished liner with 5W40 (90 µm X90 µm)	200,39	242.88
(c) Tested polished liner with rGO6 (90 µm X90 µm)	**186,75**	**199.86**
(d) Non tested polished liner (30 µm X30 µm)	6,5525	8,102
(e) Tested polished liner with 5W40 (30 µm X30 µm)	101,79	150,14
(f) Tested polished liner with rGO6 (30 µm X30 µm)	**90,034**	**101,08**
(g) Non tested polished liner (5 µm X5 µm)	6,8738	5,7373
(h) Tested polished liner with 5W40 (5 µm X5 µm)	31,66	69.669
(i) Tested polished liner with rGO6 (5 µm X5 µm)	**26,856**	**47.999**

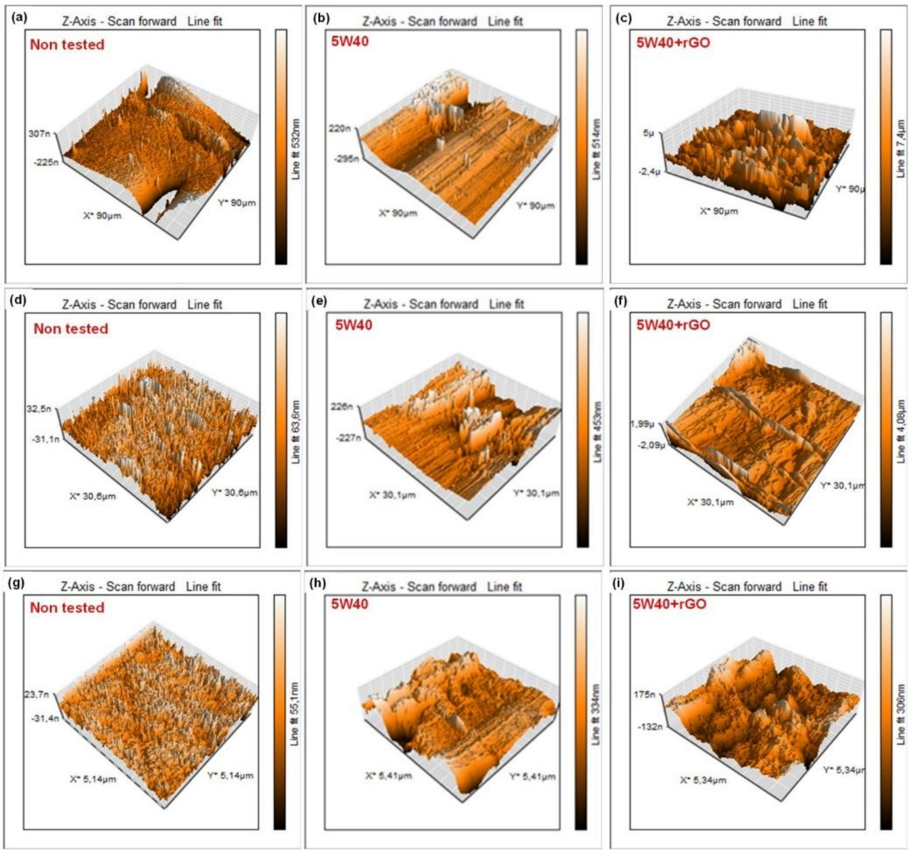

Fig. 46. 2D and 3D AFM images of the surfaces of the non-tested liner (a,d,g) and the liner tested with reference oil (b,e,h) and rGO added oil (c,f,i) at the top dead center for 3 magnifications 90 µm X90 µm, 30 µm X30 µm and 5 µm X5 µm respectively.

4. CONCLUSIONS

1. Effect of reduced graphene oxide in sample (0.02 wt.%) added into fully formulated oil using cylinder barrel of Diesel engine on friction, wear is well investigated with reciprocating tribometer and engine dynamometer.
2. It is well demonstrated that under the boundary lubrication conditions, reduced graphene oxide in sample (0.02 wt.%) added into fully formulated oil improved the frictional behavior of rubbing surfaces. Friction coefficient of ball on polished cylinder liner decreased %3.29 in comparison to the reference oil 5W40. It has been demonstrated that the wear scar diameter as well as wear scar width presented lowest values on the ball and liner tested with rGO added oil related to the reference 5W40 oil measuring with digital optical microscopic examination. The wear mechanisms of all specimens were dominantly abrasive wear mechanism.
3. It has also been measured that the roughness parameters such as Sa and Ra values were found smaller on the balls as well as polished liners tested with rGO added oil related to the reference 5W40 oil in 2D and 3D roughness measurements.
4. At the end of tribotests measurement of AFM roughness parameters such as Sa and Ra values (in nm) decreased because there is an homogeneous plastic deformation which makes the surface smooth and reactive providing better surface degradation, this allows quick surface reaction between the lubricants and sliding pairs for the test of rGO added oil because additives such as Zn, Ca, P content mixed with it and formed protective layers reducing the coefficient of friction.
5. Diesel engine presented that rGO-containing oil increased engine power by 12.01% and engine torque by 12.00% compared to the reference oil.

Acknowledgements

WE would like to thank to Dr. Minas M. Stylianakis from Institute of Electronic Structure and Laser, Foundation for Research and Technology Hellas (FORTH), GR-70013 Heraklion, Crete, Greece proving supporting us the suspension of rGO in 5W40 oil.
This research was supported by Research Fund of the Yildiz Technical University. Project ID: 3944, Project Code: FDK-2020-3944.

REFERENCES

[1] A. Kotia, S. Borkakoti, and S. K. Ghosh, "Wear and performance analysis of a 4-stroke diesel engine employing nanolubricants," *Particuology*, vol. 37, pp. 54–63, Oct. 2017, doi: 10.1016/j.partic.2017.05.016.

[2] M. Kole and T. K. Dey, "Role of interfacial layer and clustering on the effective thermal conductivity of CuO–gear oil nanofluids," *Experimental Thermal and Fluid Science*, vol. 35, no. 7, pp. 1490–1495, Jul. 2011, doi: 10.1016/j.expthermflusci.2011.06.010.

[3] M. V. Thottackkad, R. K. Perikinalil, and P. N. Kumarapillai, "Experimental evaluation on the tribological properties of coconut oil by the addition of CuO nanoparticles," *International Journal of Precision Engineering and Manufacturing*, vol. 13, no. 1, pp. 111–116, Jan. 2012, doi: 10.1007/s12541-012-0015-5.

[4] K. Holmberg and A. Erdemir, "The impact of tribology on energy use and CO2 emission globally and in combustion engine and electric cars," *Tribology International*, vol. 135, pp. 389–396, Mar. 2019, doi: 10.1016/j.triboint.2019.03.024.

[5] L. Zhou, H. Wang, and G. Sun, "Synergistic effects of graphene additives and piston ring surface treatment on friction properties of engine oil," *Physica Scripta*, vol. 99, no. 3, p. 035006, Jan. 2024, doi: 10.1088/1402-4896/ad22c3.

[6] K. Holmberg, P. Andersson, and A. Erdemir, "Global energy consumption due to friction in passenger cars," *Tribology International*, vol. 47, pp. 221–234, Dec. 2011, doi: 10.1016/j.triboint.2011.11.022.

[7] A. K. Geim and K. S. Novoselov, "The rise of graphene," *Nature Materials*, vol. 6, no. 3, pp. 183–191, Mar. 2007, doi: 10.1038/nmat1849.

[8] K. S. Novoselov *et al.*, "Electric field effect in atomically thin carbon films," *Science*, vol. 306, no. 5696, pp. 666–669, Oct. 2004, doi: 10.1126/science.1102896.

[9] X. Li *et al.*, "Large-Area synthesis of High-Quality and uniform graphene films on copper foils," *Science*, vol. 324, no. 5932, pp. 1312–1314, May 2009, doi: 10.1126/science.1171245.

[10] F. Torrisi and T. Carey, "Graphene, related two-dimensional crystals and hybrid systems for printed and wearable electronics," *Nano Today*, vol. 23, pp. 73–96, Nov. 2018, doi: 10.1016/j.nantod.2018.10.009.

[11] R. Raccichini, A. Varzi, S. Passerini, and B. Scrosati, "The role of graphene for electrochemical energy storage," *Nature Materials*, vol. 14, no. 3, pp. 271–279, Dec. 2014, doi: 10.1038/nmat4170.

[12] K.-H. Wu *et al.*, "Electron-beam writing of deoxygenated micro-patterns on graphene oxide film," *Carbon*, vol. 95, pp. 738–745, Sep. 2015, doi: 10.1016/j.carbon.2015.08.116.

[13] P. Restuccia and M. C. Righi, "Tribochemistry of graphene on iron and its possible role in lubrication of steel," *Carbon*, vol. 106, pp. 118–124, May 2016, doi: 10.1016/j.carbon.2016.05.025.

[14] Y. Xu *et al.*, "Nano-MOS2 and graphene additives in oil for tribological applications," in *Topics in mining, metallurgy and materials engineering*, 2017, pp. 151–191. doi: 10.1007/978-3-319-60630-9_6.

[15] H. Liang, Y. Bu, J. Zhang, Z. Cao, and A. Liang, "Graphene oxide film as solid lubricant," *ACS Applied Materials & Interfaces*, vol. 5, no. 13, pp. 6369–6375, Jun. 2013, doi: 10.1021/am401495y.

[16] Y. Meng, F. Su, and Y. Chen, "Supercritical fluid synthesis and tribological applications of silver nanoparticle-decorated graphene in engine oil nanofluid," *Scientific Reports*, vol. 6, no. 1, p. 31246, Aug. 2016, doi: 10.1038/srep31246.

[17] B. -g. Rosén, R. Ohlsson, and T. R. Thomas, "Wear of cylinder bore microtopography," *Wear*, vol. 198, no. 1–2, pp. 271–279, Oct. 1996, doi: 10.1016/0043-1648(96)07207-9.

[18] M. Priest and C. M. Taylor, "Automobile engine tribology — approaching the surface," *Wear*, vol. 241, no. 2, pp. 193–203, Jul. 2000, doi: 10.1016/s0043-1648(00)00375-6.

[19] B. Gupta, N. Kumar, K. Panda, S. Dash, and A. K. Tyagi, "Energy efficient reduced graphene oxide additives: Mechanism of effective lubrication and antiwear properties," *Scientific Reports*, vol. 6, no. 1, p. 18372, Jan. 2016, doi: 10.1038/srep18372.

[20] H. Kaleli *et al.*, "Tribological performance investigation of a commercial engine oil incorporating reduced graphene oxide as additive," *Nanomaterials*, vol. 11, no. 2, p. 386, Feb. 2021, doi: 10.3390/nano11020386.

[21] M. Wiśniewska, K. Terpiłowski, S. Chibowski, T. Urban, V. I. Zarko, and V. M. Gun'ko, "Stability of colloidal silica modified by macromolecular polyacrylic acid (PAA) – Application of turbidymetry method," *Journal of Macromolecular Science Part A*, vol. 50, no. 6, pp. 639–643, Jan. 2013, doi: 10.1080/10601325.2013.784562.

[22] A. Alshwawra, F. Pohlmann-Tasche, F. Stelljes, and F. Dinkelacker, "Enhancing the geometrical performance using initially conical cylinder liner in Internal Combustion Engines—A numerical study," *Applied Sciences*, vol. 10, no. 11, p. 3705, May 2020, doi: 10.3390/app10113705.

[23] S. Shahnazar, S. Bagheri, and S. B. A. Hamid, "Enhancing lubricant properties by nanoparticle additives," *International Journal of Hydrogen Energy*, vol. 41, no. 4, pp. 3153–3170, Jan. 2016, doi: 10.1016/j.ijhydene.2015.12.040.

[24] C.-G. Lee, Y.-J. Hwang, Y.-M. Choi, J.-K. Lee, C. Choi, and J.-M. Oh, "A study on the tribological characteristics of graphite nano lubricants," *International Journal of Precision Engineering and Manufacturing*, vol. 10, no. 1, pp. 85–90, Jan. 2009, doi: 10.1007/s12541-009-0013-4.

[25] N. Nyholm and N. Espallargas, "Functionalized carbon nanostructures as lubricant additives – A review," *Carbon*, vol. 201, pp. 1200–1228, Oct. 2022, doi: 10.1016/j.carbon.2022.10.035.

[26] E. Tomanik, W. Christinelli, R. M. Souza, V. L. Oliveira, F. Ferreira, and B. Zhmud, "Review of Graphene-Based Materials for Tribological Engineering Applications," *Eng—Advances in Engineering*, vol. 4, no. 4, pp. 2764–2811, Nov. 2023, doi: 10.3390/eng4040157.

[27] X. Kuang, X. Yang, H. Bian, R. Kuang, N. Hu, and S. Li, "Performance evaluation of nano-graphene lubricating oil with high dispersion and low viscosity used in diesel engines," *PLoS ONE*, vol. 19, no. 8, p. e0307394, Aug. 2024, doi: 10.1371/journal.pone.0307394.

[28] Ö. Can and Ö. Çetin, "Potential use of graphene oxide as an engine oil additive for energy savings in a diesel engine," *Engineering Science and Technology an International Journal*, vol. 48, p. 101567, Nov. 2023, doi: 10.1016/j.jestch.2023.101567.

[29] E. Tomanik *et al.*, "Effect of graphene nanoplatelets as lubricant additive on fuel consumption during vehicle emission tests," *Preprints.org*, Dec. 2024, doi: 10.20944/preprints202412.0909.v1.

[30] G. Koszalka, E. Tomanik, T. M. Maria, W. Christinelli, and W. Grabon, "Effect of graphene as a lubricant additive for diesel engines," *Energies*, vol. 18, no. 2, p. 257, Jan. 2025, doi: 10.3390/en18020257.